Design and Analysis of an On-Board Electric Vehicle Charger for Wide Battery Voltage Range

Nihar Ranjan Mohanty

Department of Electrical Engineering

National Institute of Technology Rourkela

DESIGN AND ANALYSIS OF AN ON-BOARD ELECTRIC VEHICLE CHARGER FOR WIDE BATTERY VOLTAGE RANGE

Thesis submitted in partial fulfillment

of the requirements of the degree of

Masters of Technology

in

Electrical Engineering

by

Nihar Ranjan Mohanty

(Roll no. 214EE5261)

based on the research carried out

under the supervision of

Prof. Sanjeeb Mohanty

Department of Electrical Engineering

National Institute of Technology Rourkela

May 2016

Department of Electrical Engineering

National Institute of Technology Rourkela

May 18, 2016

Certificate of Examination

Roll Number: 214EE5261

Name: Nihar Ranjan Mohanty

Title of Thesis: Design and analysis of an on-board electric vehicle charger for wide battery voltage range

I, the below signed, after checking the thesis mentioned above and the official record book(s) of the student, hereby state my approval of the thesis submitted in partial fulfillment of the requirements for the degree of ***Master of Technology*** in ***Department of Electrical Engineering*** at ***National Institute of Technology Rourkela***. I am satisfied with the volume, quality, correctness, and originality of the work.

……

Prof. Sanjeeb Mohanty

Principal Supervisor

Department of Electrical Engineering

National Institute of Technology Rourkela

Prof. Sanjeeb Mohanty

Department of Electrical Engineering

May 18, 2016

Supervisor's Certificate

This is to certify that the work presented in this thesis entitled **"*Design and analysis of an on-board electric vehicle charger for wide battery voltage range*"** by **"*Nihar Ranjan Mohanty*"** Roll Number **214EE5261** is a record of original research carried out by him under my supervision and guidance in partial fulfilment of the requirements for the degree of ***Master Of Technology*** in ***Department of Electrical Engineering***. Neither this thesis nor any part of it has been submitted for any degree or diploma to any institute or university in India or abroad.

……

Prof. Sanjeeb Mohanty

DECLARATION OF ORIGINALITY

I, Nihar Ranjan Mohanty, Roll no. 214EE5261 hereby declare that this thesis entitled ''***Design of an On-Board Electric Vehicle Charger for Wide Battery Voltage Range***'' represents my original work carried out as a postgraduate student of NIT Rourkela and, to the best of my knowledge, it contains no material previously published or written by another person, nor any material presented for the award of any other degree or diploma of NIT Rourkela or any other institution. Any contribution made to this research by others, with whom I have worked at NIT Rourkela or elsewhere, is explicitly acknowledged in the thesis. Works of other authors cited in this thesis have been duly acknowledged under the section "References". I have also submitted my original research records to the scrutiny committee for evaluation of my thesis.

I am fully aware that in the case of any non-compliance detected in future, the Senate of NIT Rourkela may withdraw the degree awarded to me on the basis of the present thesis.

May 18, 2016

NIT Rourkela **Nihar Ranjan Mohanty**

ACKNOWLEDGEMENTS

In the pursuit of academic endeavor, I feel I have been singularly fortunate. Firstly, I would like to express my sincere gratitude to my advisor **Prof. Sanjeeb Mohanty** for the continuous support of my M.Tech research, for his patience, motivation, and immense knowledge. His guidance helped me in all the time of research and writing of this thesis. I could not have imagined having a better advisor and mentor for my M.Tech study.

I owe a depth of gratitude to **Prof. Jitendriya Kumar Satapathy,** H.O.D. Department of Electrical Engineering, National Institute of Technology Rourkela and all the other faculties for the facilities provided during my study.

I would like to express my profound gratitude to my parents, my family, and friends who have always given me their love, encouragement, and endless support throughout these years.

Place: NIT Rourkela

Date: 18.05.2016 Nihar Ranjan Mohanty

ABSTRACT

The scarcity of fossil fuel and the increased pollution leads the use of Electric Vehicles (EV) and Hybrid Electric Vehicles (HEV) instead of conventional Internal Combustion (IC) engine vehicles. An Electric Vehicle requires an on-board charger (OBC) to charge the propulsion battery. The objective of the project work is to design a multifunctional on-board charger that can charge the propulsion battery when the Electric Vehicle (EV) connected to the grid. In this case, the OBC plays an AC-DC converter. The surplus energy of the propulsion battery can be supplied to the grid, in this case, the OBC plays as an inverter. The auxiliary battery can be charged via the propulsion battery when PEV is in driving stage. In this case, the OBC plays like a low voltage DC-DC converter (LDC). An OBC is designed with Boost PFC converter at the first stage to obtain unity power factor with low Total Harmonic Distortion (THD) and a Bi-directional DC-DC converter to regulate the charging voltage and current of the propulsion battery. The battery is a Li-Ion battery with a nominal voltage of 360 V and can be charged from depleted voltage of 320 V to a fully charged condition of 420 V. The function of the second stage DC-DC converter is to charge the battery in a Constant Current and Constant Voltage manner. While in driving condition of the battery the OBC operates as an LDC to charge the Auxiliary battery of the vehicle whose voltage is around 12 V. In LDC operation the Bi-Directional DC-DC converter works in Vehicle to Grid (V2G) mode. A 1KW prototype of multifunctional OBC is designed and simulated in MATLAB/Simulink. The power factor obtained at full load is 0.999 with a THD of 3.65 %. The Battery is charged in A CC mode from 320 V to 420 V with a constant battery current of 2.38 A and the charging is switched into CV mode until the battery current falls below 0.24 A. An LDC is designed to charge a 12 V auxiliary battery with CV mode from the high voltage propulsion battery.

Keywords: Bi-directional DC-DC converter; Boost PFC converter; electric vehicle; low voltage DC-DC converter; vehicle-to-grid.

CONTENTS

Certificate of examination ii
Supervisor's certificate iii
Declaration of originality iv
Acknowledgements v
Abstract vi
Contents vii
List of figures ix
List of tables x
Abbereviations xi
1 Introduction
1.1 Background 1
1.2 Electric Vehicle vs. Hybrid Electric Vehicle 2
1.2 Battery Chargers for Plug-In Electric Vehicles 3
1.3 Battery study 3
1.3.1 Introduction 3
1.3.2 Electrical Model of Li-Ion Battery 4
1.3.3 Charging profile of Li-Ion Battery 5
1.4 Charger infrastructure and power levels 5
1.5 Literature Review 6
1.6 Motivation 8
1.7 Objective 8
1.8 Organization of Thesis 9
1.9 Conclusion 9
2 Front-end AC-DC converter
2.1 Introduction 10
2.2 Basic Definitions 10
2.3 Harmonic standards 12
2.4 Diode Rectifier 14
2.4.1 with C filter 14
2.4.2 With LC filter 16
2.5 Active PFC Converter 18
2.6 Boost PFC Converter 19
2.6.1 Switching operation of Boost converter 19
2.6.2 Different modes of operation 21

2.6.3 CCM Boost PFC Converter Design 22
2.7 Controller Design 24
2.7.1 Current Controller 25
2.7.2 Voltage Controller 27
2.8 Simulation and Results 27
2.9 Conclusion 30
3 Back-end DC-DC converter
3.1 Introduction 31
3.2 Non-Isolated Bidirectional DC-DC Converter 32
3.2.1 Bidirectional Half Bridge DC-DC Converter 32
3.2.1.1 G2V Mode 33
3.2.1.2 V2G Mode 35
3.4 State Space Averaging 35
3.4.1 G2V Mode 37
3.4.2 V2G Mode 40
3.5 Design of Controller 41
3.5.1 G2V operation 41
3.5.1.1 Voltage Controller Design 42
3.5.1.2 Current Controller Design 44
3.5.2 V2G operation 44
3.6 Low Voltage DC-DC Converter 45
3.6.1 Power Stage Design and Operation of LDC 46
3.6.2 Controller Design of LDC 47
3.7 Simulation and Results 47
3.7.1 G2V Mode 47
3.7.2 V2G Mode 48
3.7.3 LDC 49
3.8 Conclusion 50
4 Conclusion and future scope
4.1 Conclusion 51
4.2 Future Scope 51
References 52

LIST of FIGURES

1.1 Block diagram of electric vehicle 2
1.2 Block diagram of hybrid electric vehicle 2
1.3 Block diagram of EV charger 3
1.4 Equivalent model of Li-Ion battery 4
1.5 Charging characteristics of Li-ion cell 5
2.1 Diode bridge rectifier (a) power stage diagram (b) output voltage (VS=230 V RMS) 14
2.2 Diode rectifier with C filter (a) power stage diagram(b)output voltage(c)input current(VS=230 V RMS and C =200µF) 15
2.3 Diode rectifier with C filter (a) input current FFT analysis (b) rectified voltage capacitor voltage and input current (input current is magnified by ten times for better visibility) 16
2.4 Diode rectifier with LC filter (a) input current (b) FFT of input current(L= 20 mF and C=200µF) 17
2.5 Filter inductance versus THD graph 18
2.6 Block Diagram of Active PFC 18
2.7 Boost PFC converter 19
2.8 (a) Boost converter and equivalent circuit during (b) ON interval (c) OFF interval 20
2.9 Inductor current in (a) CCM (b) DCM 22
2.10 Boost PFC converter with ACM controller 24
2.11 Current loop block diagram 25
2.12 Bode plot of plant and plant with current controller 26
2.13 Boost PFC results for 1000 W load (a) input voltage and current (scaled ten times) and output voltage, (b) THD of input current$LB = 1mF, CDC = 700\ \mu F, fsw = 200kHz, Vs = 230\ V\ rms$ 28
2.14 Boost PFC converter operating at Half-Load output voltage, input voltage and current(scaled ten times for better visibility) of Boost PFC converter operating at Half-Load $LB = 1mF, CDC = 700\ \mu F, fsw = 200kHz, Vs = 230\ V\ rms$ 29
2.15 Input current and output current when a step load changes from 500 W to 1000 W. 29
3.1 Non-isolated Half-Bridge DC-DC Converter 33
3.2 Half-Bridge DC-DC Converter (a) G2V mode (b) V2G mode 34
3.3 G2V operation (a) ON interval (b) OFF interval 34
3.4 Buck Converter (a) ON interval (b) OFF interval 37
3.5 Controller for DC-DC converter in G2V operation 41
3.6 Bode plot of the plant with and without controller 43
3.7 Controller for V2G mode 44
3.8 Block Diagram of Power distribution in EV 45
3.9 Low-Voltage DC-DC converter 46
3.10 Simulated Results of Charging operation of the propulsion battery (a)Voltage and (b)Current in Beginning Point(c)voltage and (d)current in Nominal Point (e)voltage and (f)current in Turning Point(g)voltage and (h)current in End Point 48
3.11 DC link voltage and current during G2V operation (The current is multiplied by 100 for batter visibility) 49
3.12 Voltage and Current of Auxiliary battery during charging 49

LIST of TABLES

Table 1.1	Technical specifications of Mahindra Reva	1
Table 1.2	Charging power levels and rating of EV	6
Table 2.1	IEC 61000-3-2 standard for class a equipment	12
Table 2.2	Voltage harmonic limits	13
Table 2.3	Current harmonic limits	13
Table 2.4	AC-DC PFC converter specifications	23

ABBREVIATIONS

AC	Alternating Current
ACM	Average Current Mode
BCM	Boundary Conduction Mode
BW	Band Width
CC	Constant Current
CCM	Continuous Conduction Mode
CV	Constant Voltage
DC	Direct Current
DCM	Discontinuous Conduction Mode
EV	Electric Vehicle
G2V	Grid to Vehicle
HEV	Hybrid Electric Vehicle
IEC	International Electro-technical Commission
IEEE	Institute of Electrical and Electronics Engineers
LDC	Low Voltage DC-DC Converter
MOSFET	Metal Oxide Semiconductor Field Effect Transistor
OBC	On-Board Charger
PCC	Point of Common Coupling
PCM	Peak Current Mode
pf	Power Factor
PFC	Power Factor Correction
PM	Phase Margin
PWM	Pulse Width Modulation
RMS	Root Mean Square
TDD	Total Demand Distortion
THD	Total Harmonic Distortion
V2G	Vehicle to Grid
ZCS	Zero Current Switching
ZVS	Zero Voltage Switching

CHAPTER 1

INTRODUCTION

1.1 Background

Conventional Internal Combustion (IC) engine vehicles use petroleum products (i.e. petrol, diesel, or LPG) as the source of energy for driving purpose. The shortage of fossil fuel is the most critical issue over worldwide and the immediate solution is to minimize the use of fossil fuel as much as possible. Moreover, conventional IC engine vehicles emit carbon dioxide and various greenhouse gasses by making it harder to satisfy environmental regulations. The solution leads to adopting alternate fuel vehicles such as Electric Vehicles (EV) and Hybrid Electric Vehicle (HEV). EV does not emit tailpipe pollutant like particulates, ozone, volatile organic compounds, carbon monoxide, hydrocarbons, lead and oxides of nitrogen which plays a vital role in air pollution and greenhouse gas Moreover the fossil fuel issue can be minimized.

As of September 2015 around 30 models of commercial electric cars and utility vans are launched mainly in China, United States, Western European countries and Japan. Over 620,000 light-duty electric vehicles have been sold by mid of September 2015 [1].Some of the EV manufacturers are BMW, Nissan, Mahindra, Tesla motor etc. Table 1.1 shows the technical specification of an EV from Mahindra. As in one full charge the vehicle produces a range of 120 Km, hence, EV can be adapted for commercial usage.

Table 1.1 Technical specifications of Mahindra REVA

Parameter	Value
Power	19 kW @ 3750 rpm
Torque	53.9 N-m @ [0-3400] rpm
Battery	48 V Li-ion
Range	120 km in one full charge
Charging time	5 hours from a 220 V,15 A socket

(http://mahindrareva.com/product/specifications)

1.2 Electric Vehicle vs. Hybrid Electric Vehicle

Electric vehicles have only one source of energy i.e. the on-board battery bank and by utilizing the stored energy, they drive the vehicle. The battery bank can be charged by taking electricity from either conventional or non-conventional sources. The schematic shows the block diagram of an electric vehicle. As shown in the figure the power electronic converter matches the electrical ratings of the battery bank and the motor. The motor can be a DC motor or AC motor, depending on the motor the converter can be a DC-DC converter or DC-AC converter. Large charging time, limited range of driving due to the limited capacity of the on-board battery pack are the challenges that can be considered [2].

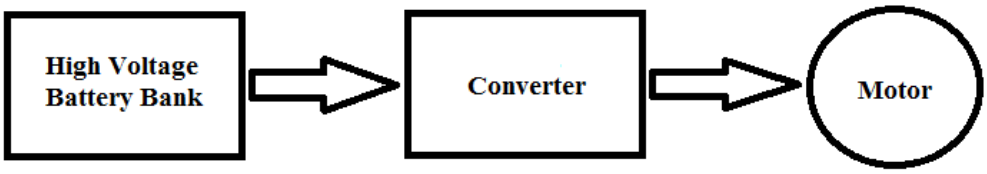

Fig 1.1 Block diagram of electric vehicle

Unlike EVs hybrid electric vehicles (HEV) have two or more sources of energy. The sources can be a battery bank and a fuel cell or an IC engine along with a battery bank.Fig.1.2 shows the block diagram of an HEV. It can be observed from the block diagram that both the IC engine and the Battery bank van be utilized to drive the vehicle hence by improving the range of the vehicle [3].

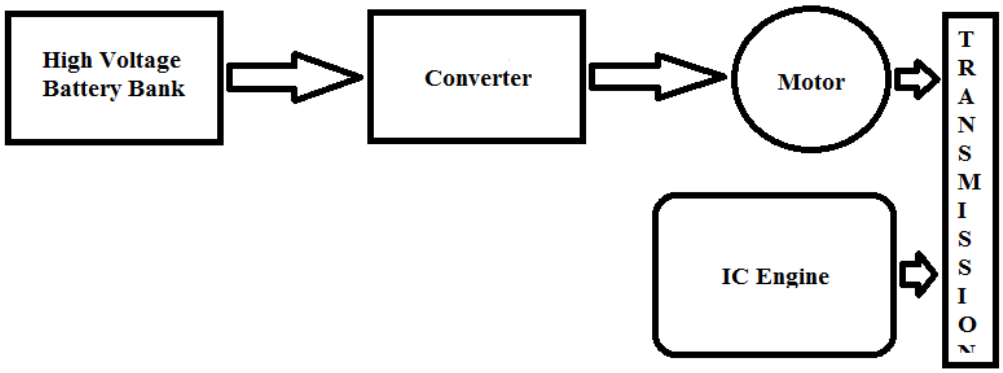

Fig 1.2 Block diagram of hybrid electric vehicle

1.2 Battery Chargers for Plug-In Electric Vehicles

In order to utilize the battery to its maximum capacity the battery charger plays a crucial role. The remarkable features of a battery charger are efficiency and reliability, weight and cost, charging time and power density. The characteristics of the charger depend on the components, switching strategies, control algorithms. This control algorithm can be implemented digitally using micro-controller [4].

The figure below shows the block diagram of an EV charger. The charger consists of two stages. First, one is the AC-DC converter with power factor correction which converts the AC grid voltage into DC ensuring high power factor and low THD. The later stage regulates the charging current and voltage of the battery according to the charging method employed.

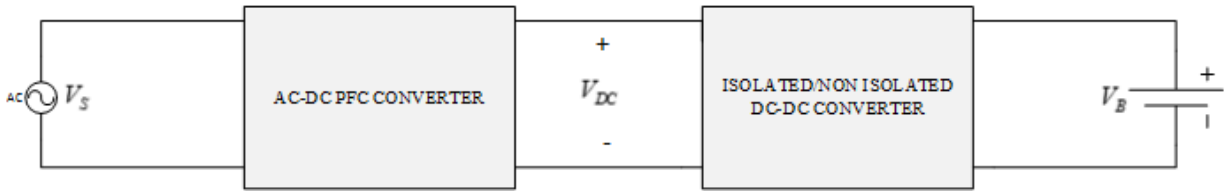

Fig 1.3 Block diagram of EV charger

The charger can be unidirectional i.e. can only charge the EV battery from the grid or bidirectional i.e. can charge the battery from the grid in charging mode and can pump the surplus amount of power of the battery into the grid. Both isolated and non-isolated topologies can be employed for the charger. The details of each stage are thoroughly described in subsequent chapters.

1.3 Battery study

1.3.1 Introduction

The very first step of designing an Electric Vehicle (EV) or Hybrid Electric Vehicle (HEV) is to design the suitable propulsion battery which is responsible for driving the motor. The battery must be able to satisfy the electric specifications such as operating voltage, power, power and energy densities and long working cycle and life.

Presently Lithium-Ion battery is the most commonly used in automobile industries. The advantages of Li-Ion battery are listed below

1. The energy density of Li-Ion battery is around twice of Ni-Cd battery and the load characteristics are almost similar as Ni-Cd battery.

2. A single cell of Li-Ion battery is of 3.6 volts where it is 1.2 volts and 2 volts in the case of Ni-Cd and Lead Acid battery respectively.

3. The discharge rate of the battery is fairly flat i.e. it delivers a constant power over 80% of the discharge cycle.

4. The weight of Li-ion battery pack is much less than Ni-Cd. For example 20kWh Li-ion battery pack weights around 160 kg while Ni-Cd weights around 275-300 kg for the same ratings.

With above advantages, Li-ion batteries also have some major drawbacks which are the battery is very costly, flammable and the life cycle is limited between 400 and 700 cycles. The safety issue can be eliminated by using Lithium ion phosphate batteries which life cycle is around 1000 cycles.

1.3.2 Electrical Model of Li-Ion Battery

The main objective to model a battery is to represent the battery operation via a mathematical equation or equivalent circuit or both. Equivalent circuit model is convenient for power system simulations as it can be modeled with basic electrical components such as voltage source, resistor, and capacitors.

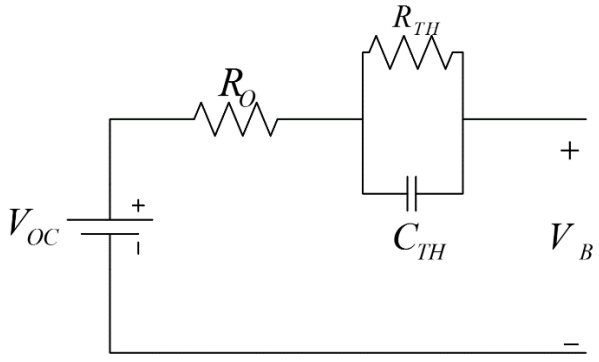

Fig 1.4 Equivalent model of Li-Ion battery

The above figure shows the Thevenin's equivalent model of a Li-Ion battery. The open circuit voltage is V_{oc}. Both ohmic resistance R_o and polarization resistance R_{Th} are

accounted for internal resistance and the transient response during charging are discharging are modelled by an equivalent capacitanceC_{Th}. V_B represents the effective battery voltage.

1.3.3 Charging profile of Li-Ion Battery

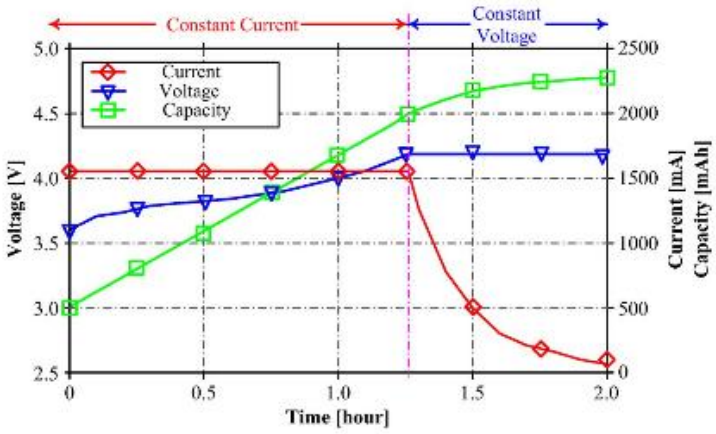

Fig 1.5 Charging characteristics of Li-ion cell

The CC/CV mode charging is most commonly used for Li-ion battery. Fig 1.5 shows the charging characteristics of a single Li-ion cell with a nominal voltage of 3.6 V during charging. Four key points can be marked during the charging process [5]. The beginning and end point related to the starting and termination of the charging. The nominal point where the battery voltage equals to the nominal voltage and the turning point where the charging mode is converted from CC to CV. The depleted voltage of the Li-ion cell is below the nominal voltage of the cell. First, the battery is charged in a CC mode up to the turning point where the battery voltage reached s to the maximum voltage with 100% SoC the battery is charged with CV mode toil the charging current falls below a permissible limit.

1.4 Charger infrastructure and power levels

The total amount of power that can be transferred, charging time, cost, location and effect on the grid are some important features of the charger. Some important issues like charging time, standardization of charging stations, distribution, and demand policies can be addressed by the deployment of charging infrastructure and electric vehicle supply equipment (EVSE) [6].

Based on power levels the chargers are classified into three categories and are described below.

Level 1 charging:

It is the slowest method and according to U.S. standard 120 V/15A single phase outlet can be used for the charging purpose. A standard J1772 connector can be used to connect the EV ac port with the charging outlet. No extra infrastructure is necessary and the vehicle can be charged in home or office overnight. The charger is an on-board charger (OBC) i.e. the charger can be mounted inside the vehicle.

Level 2 charging:

It is the semi-fast charging method. According to U.S. standards, a 240 V outlet is necessary for level 2 charging. Dedicated equipment may be required at home or office for this charging method.

Level 3 charging:

Generally, level 3 charging offers DC fast charging or AC fast charging ad the time taken is less than 1 hour. Dedicated charging stations are required and an off-board charger is employed to convert the AC power into DC in order to charge the battery.

The details of the charging levels and connectors are listed in the table below:

Table 1.2 Charging power levels and rating of EV

Power level types	**Voltage and current ratings**	**Expected power level**	**Connector**
Level 1	120 V/15 A	2 k W	SAEJ1772,NEMA 5-15
Level 2	240 V/(12-80) A	2.9-19.2 kW	SAEJ1772,IEC62196
Level 3	400 V AC/(32-63) A	22.1-43.7 kW	EC 60309

1.5 Literature Review

The charger in [7] requires a four switch AC-DC converter for PFC operation and a full bridge DC-DC converter for CC/CV mode charging operation. The PFC controller is designed with battery voltage and current references i.e by making the control circuit more complex.

A level 2 charger combining bridgeless boost PFC converter as front-end converter and isolated phase shifted full bridge DC-DC converter is presented in [8].To obtain high density and high-efficiency silicon carbide power switches(SiC) are utilized. A maximum efficiency of 95 % and minimum THD 4.2 % is obtained at a frequency of 200 kHz.

Smart Homes and Smart Grid based operation modes for EV is described in [9].Usually, two modes of power transfer occur between EV and Grid i.e. Grid to Vehicle and Vehicle to Grid. The literature proposes additional two modes namely Vehicle for Grid and home to Vehicle. A Vehicle to Home operation is proposed. In H2V mode, the charger current is controlled depending on the in home appliances and their consumption of power.V4G operation is aimed for the reactive power compensation in the home itself with the utilization of the vehicle charger. In V2H mode, the vehicle supplies power to a single home unlike in V2G mode where the vehicle is supposed to supply power to the grid. A 3.6 kW charger prototype is developed with bi-directional power flow capabilities to achieve all modes of operations.

In [10] an on-board battery charger for the electric scooter is developed. The charger is designed for a lead-acid battery of 180 V and 12 Ah and the charger can charge the battery from an 110 V, 60 Hz, single phase outlet. The concept of low voltage DC-DC converter (LDC) is proposed. In order to charge a 12 V auxiliary battery from the 180 V propulsion battery, a DC-DC converter is proposed.

A resonant synchronous DC-DC converter operating in DCM is proposed in [11].The required amount of dead time and reversed current for DCM operation can be calculated for a ZVS operation in the entire range of operation. The parameter selections can be directly done from the datasheets of the components without performing any simulation or experimental verification.

Different PFC topologies which include Diode Bridge at first stage followed by Buck, Boost, Buck-Boost, SEPIC can be used to feed Brush Less DC Motors. In [12] different topologies are simulated and analyzed in order to choose appropriate topology for the desired application. The paper suggests diode bridge rectifier based PFC topologies are best choice for low power applications. Boost PFC topology make an advantage where output DC voltage more than input is desired. When output DC voltage less than RMS value of input AC voltage is essential Buck based PFC topologies are suitable. Buck-Boost derived topologies like Cuk, SEPIC are drawn an advantage where power less than 500 W

is desired. Half Bridge and Push Pull topologies have low THD with the medium power of operation than Boost PFC converter. However, the component count increases and the selection should be based on the trade-off between performance and cost and complexity.

A Buck PFC converter with Constant on-time control has been proposed in [13].The experimental validation of the proposed design is carried out for 100 W power with a supply of 90 V. The design meets the IEC61000-3-2 harmonic standards. The efficiency is calculated as 0.96 with a full load and universal voltage operation. The main disadvantage of Buck type PFC converter is the discontinuous input current, which requires a large filter at the input.

A novel two-switch Boost-interleaved buck-boost topology has been proposed in [14].The designed converter having an advantage of less voltage stress on the switches and reduced conduction loss in switch and inductor with reduced size. An efficiency of 93 % is obtained during universal line voltage input with low THD.

1.6 Motivation

As the world is moving towards alternate fuel vehicles, EVs and HEVs can be adopted to restrict the usage of fossil fuel and increased environmental pollutions. Most of the EVs have a lower driving range for which a frequent charging process is essential. The charger must be compatible enough so that it can be mounted on the vehicle itself and the vehicle can be charged when the suitable outlet is available.

1.7 Objective

The objective of this thesis work is to provide an On-Board EV charger for level 1 charging purpose. The designed OBC is a two stage charger with Boost PFC converter at the front end for conversion of AC to DC with very high PF whereas the second stage is a Non-Isolated DC-DC converter for battery voltage and current regulation.

The high voltage propulsion battery is considered as a Li-Ion type and CC/CV charging algorithm is developed for the battery. An LDC is designed with the utilization of the OBC for charging the Auxiliary battery from the propulsion battery.

1.8 Organization of Thesis

The thesis is organized in the following manner

Chapter 2 described the Front end AC-DC converter which is required to convert the grid voltage into a suitable DC voltage with low current harmonic and thus by ensuring a high power factor.

Chapter 3 explains the second stage of an OBC i.e. a DC-DC converter to regulate the charging current and voltage. Furthermore, a Vehicle-to-Grid mode operation of the DC-DC converter is presented. An LDC is designed and analyzed to charge the auxiliary battery from the propulsion battery by utilizing the designed OBC.

Chapter 4 deals with the overall concluding points of the designed EV charger for charging both propulsion battery and auxiliary battery. The next design aspects of the OBC is stated in this chapter.

1.9 Conclusion

The basic difference between EV and HEV is stated in 1.1 of this chapter. A brief explanation of two stage EV charger with the power converters required for each stage is described in 1.2.New era EVs and HEVs use high voltage Lithium Ion battery pack for driving purpose. The various advantages of Li-ion battery and the charging profile i.e. CC/CV mode charging which is suggested by the battery manufacturers and the equivalent electrical model of the battery are thoroughly explained in 1.3.section 1.5 describes different classifications of EV charger based on the power levels and power flow capability i.e. unidirectional and bidirectional. In 1.5 previous work regarding EV charger and the converters associated with the charger has been stated. As the first stage of an OBC is the AC-DC converter, hence, the AC-DC converter topology is explained in chapter 2.The conventional Diode Bridge Rectifier with its associated key issues are presented and the solution to the difficulties are addressed.

CHAPTER 2

FRONT-END AC-DC CONVERTER

2.1 Introduction

The Electric Vehicle can be charged from a suitable outlet via an OBC the AC-DC converter or rectifier is the first stage of an OBC which converts the available AC supply into DC.A constant voltage with less ripple at the output terminals of the AC-DC converter is desired which can be further utilized by the load or any other converter. Most common rectifier topology is Diode bridge rectifier with capacitive filter and phase controlled rectifiers. The first one is preferred for low power applications where the later one is for high power applications and three phase applications.

One most serious issue with the conventional rectifiers is the harmonics components of the line current which are responsible for distorting the voltage at the point of common coupling due to source inductance and produce some undesirable effects. Due to the presence of harmonics, the power factor becomes worst. The effect of low PF and high THD are described in section 2.2.

2.2 Basic Definitions

Power factor (pf) simply defined as the ratio of real power to apparent power. The instantaneous product of voltage and current over one complete cycle gives the real power where the product of RMS voltage and RMS current gives the apparent power.

The cosine of the angle between voltage phasor ad current phasor is defined as PF. But this definition is not valid everywhere, especially at nonlinear loads. The definition is limited up to resistive, inductive, or capacitive loads[15].

Consider a non-linear load connected with a sinusoidal voltage source. The voltage and current can be expressed as v(t) and i(t).

v(t)=$V_m sin\omega t$ and i(t)=$I_O + \sum_{n=1}^{\infty} I_n \sin(n\omega t + \emptyset_n)$ (2.1)

$V_m$is the maximum value of supply voltage. I_n is the maximum value of n^{th} harmonics component of current and $\emptyset_n$is the n^{th}harmonic phase displacement.

RMS value of current can be expressed as

$$I_{RMS} = \sqrt{I_O^2 + \sum_{n=1}^{\infty} I_n^2} \quad (2.2)$$

Power factor can be expressed as the product of displacement factor and distortion factor.

The displacement factor can be defined as the cosine of angle between fundamental component of voltage and current and as denoted by $k_{\emptyset}$.

$$k_{\emptyset} = cos\emptyset \quad (2.3)$$

Where $\emptyset$ is the phase displacement between fundamental voltage and current.

The distortion factor can be defined as the ratio of fundamental component of current to the RMS current and is denoted as k_d.

$$k_d = \frac{I_{1(RMS)}}{\sqrt{I_O^2 + \sum_{n=1}^{\infty} I_n^2}} \quad (2.4)$$

The Total Harmonic Distortion can be calculated as

$$\text{THD (\%)} = \frac{1}{\sqrt{k_d^2 - 1}} \quad (2.5)$$

Power factor can be defined as the product of displacement factor and distortion factor.

$$\text{pf} = k_d \times k_{\emptyset} \quad (2.6)$$

When the fundamental component of current is in phase with the voltage, the displacement factor is 1 and the PF $= k_d$.

$$\text{pf} = \frac{1}{\sqrt{1 + \left(\frac{THD(\%)}{100}\right)^2}} \quad (2.7)$$

Effects of current Harmonics:

- The current harmonics distorts the grid voltage at Point of Common Coupling (PCC) via line impedance of the power system and the distorted voltage cause malfunction in various electrical equipment connected to the grid.
- In AC machines, a fundamental component of current is useful and desired to produce required amount of power. Harmonic current add to the fundamental and result in increased current which in turn increases the losses in distribution transformer and AC

machines. Due to additional loss machines undergo overheating and cannot be used up to their actual rating.

- Large neutral current flows in the power system due to triple harmonics.
- Malfunctions in protection system caused by the current harmonics.

Effects of low pf:

- At low pf, the load draws more current and the loss in the converter and the transmission system increases and efficiency reduces.
- The Reactive power increases which increase the rating of the electrical components and additional reactive power has to be supplied by shunt elements or generator.

2.3 Harmonic standards

Due to the adverse effects of the harmonics, various agencies have adopted standards i.e. the maximum allowable harmonic current that can be injected into the power system by any load. A few standards are listed below.

IEC 61000-3-2 Standard:

Table 2.1 IEC 61000-3-2 standard for Class A equipment

Harmonic Number(n)	Maximum permissible current(A)
3	2.30
5	1.14
7	0.77
9	0.40
11	0.33
13	0.21
15-39	0.15

IEC stands for International Electrotechnical Commission and enforced in Europe. It defines a limit for current harmonics of equipment with a maximum input current of 16 A. The standard applies to both single phase, and three phase equipment, and the frequency may be 50 Hz or 60 Hz. Harmonic limits for Class A equipment is shown in Table 2.1.Some examples of class An equipment are rectifiers for office and computer.

IEEE Standard:

According to IEEE, the current harmonics are measured by the ratio of load current to the short circuit current. This ratio can also define as the ratio of load kVA to short circuit kVA at PCC.

The voltage harmonics distortion on the power system is limited to 5 % THD with voltage rating up to 69 kV and the current harmonics depend on the short circuit capacity of the line at PCC according to IEEE standard 519 [16].

Table 2.2 Voltage harmonic limits

Voltage at PCC	**THD limit (%)**	**Individual harmonic limit (%)**
<69 kV	5.0	3.0
69 kV-161 kV	2.5	1.5
>161 kV	1.5	1.0

Table 2.3 Current harmonic limits

I_{SC}/I_L	**h<11**	**11≤h<17**	**17≤h<23**	**23≤h<35**	**h>35**	**TDD (%)**
<20	4.0	2.0	1.5	0.6	0.3	5.0
20<50	7.0	3.5	2.5	1.0	0.5	8.0
50<100	10.0	4.5	4.0	1.5	0.7	12.0
100<1000	12.0	5.5	5.0	2.0	1.0	15.0
>1000	15.0	7.0	6.0	2.5	1.4	20.0

Where, I_{SC}/I_L maximum harmonic current distortion in percent of I_L.

h = the harmonic order (odd harmonics).

I_{SC} = short circuit current at PCC.

I_L = fundamental component of load current at PCC.

TDD=Total demand distortion.

PCC=Point of common coupling.

2.4 Diode Rectifier

One of the commonly used AC-DC converters is a diode bridge rectifier for low power applications. Fig 2.1(a) shows a diode bridge rectifier without any filter. The operation of the converter is very simple. Diagonal diodes D_1 and D_2 conduct for positive half cycle of the supply voltage and similarly diodes $D_3$and D_4 conducts for negative half of the supply voltage. The rectifier behaves as a pure resistive load to the input AC source and, the input current is in phase with the voltage, providing unity power factor operation.

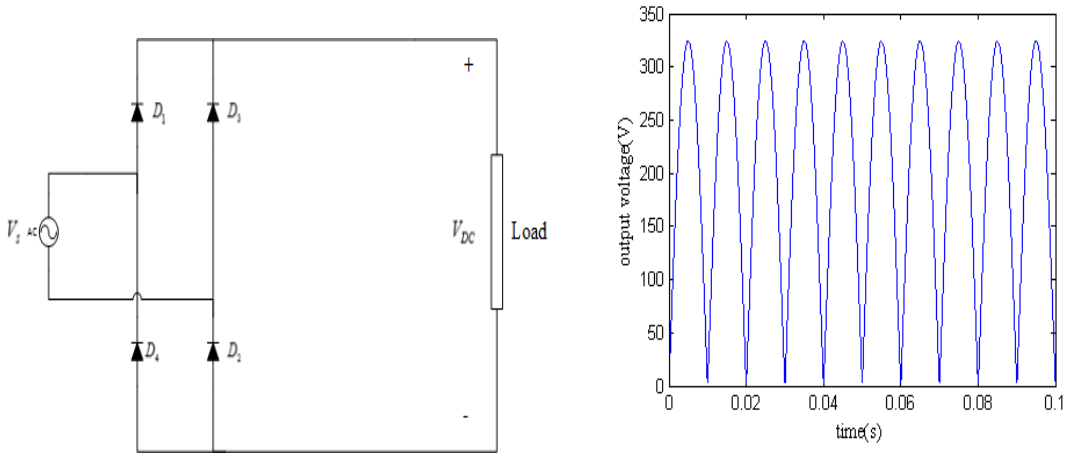

(a) (b)

Fig 2.1 Diode bridge rectifier (a) power stage diagram (b) output voltage (V_S=230 V RMS)

From the Fig 2.1(b) it can be observed that the output voltage of rectifier or load voltage V_{DC} is the rectified sine wave but the ripple in the load voltage is very high which should be minimized. In most cases the output of the rectifier is a DC-DC converter which accept an input DC voltage of a ripple within permissible limit. To reduce the ripple of the output voltage various filters are implemented which are discussed below.

2.4.1 with C filter

In order to minimize the ripple voltage at the output and maximize the average output voltage, filters are added to the conventional rectifier. A capacitive filter is one of the basic filters and widely used one. Fig 2.2(a) shows a diode bridge rectifier with C filter. Usually, the value of the capacitor is decided by the amount of allowable ripple in output voltage.

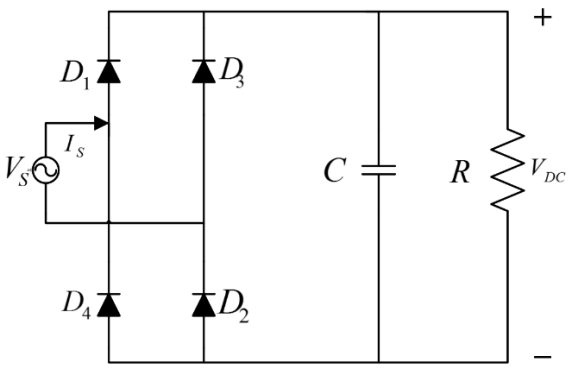

(a)

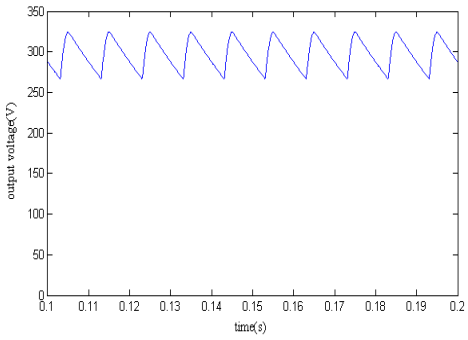

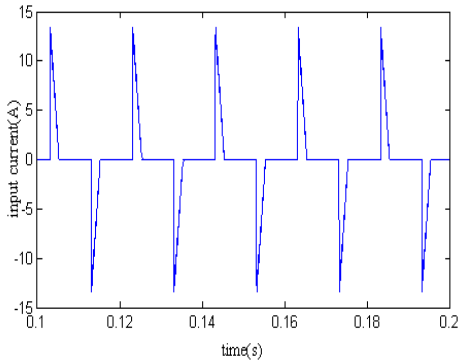

(b) (c)

Fig 2.2 Diode rectifier with C filter (a) power stage diagram(b)output voltage(c)input current(V_S=230 V RMS and C =200µF)

As shown in Fig 2.2 (b) the voltage is having a ripple of 60 V peak-to-peak. The ripple can be minimized further by increasing the value of filter capacitor. The input current is not sinusoidal, but it contains harmonics that can be verified from the FFT of the input current in Fig 2.3(a).The input current is discontinuous i.e. the diagonal diodes does not conduct for the entire half cycle of the supply. With the increase in the capacitance value, the conduction period of the diodes decreases and the input current peak increases with the increase in THD. The reason for the momentary current is explained below.

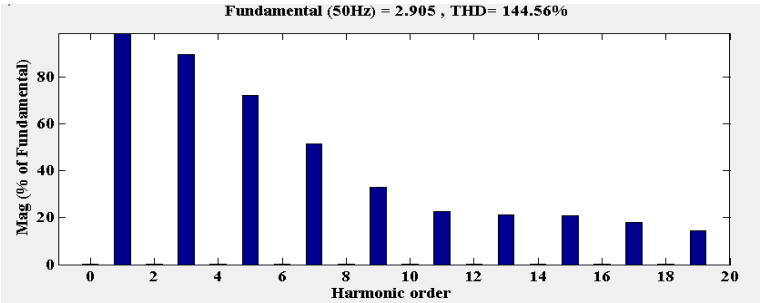

(a)

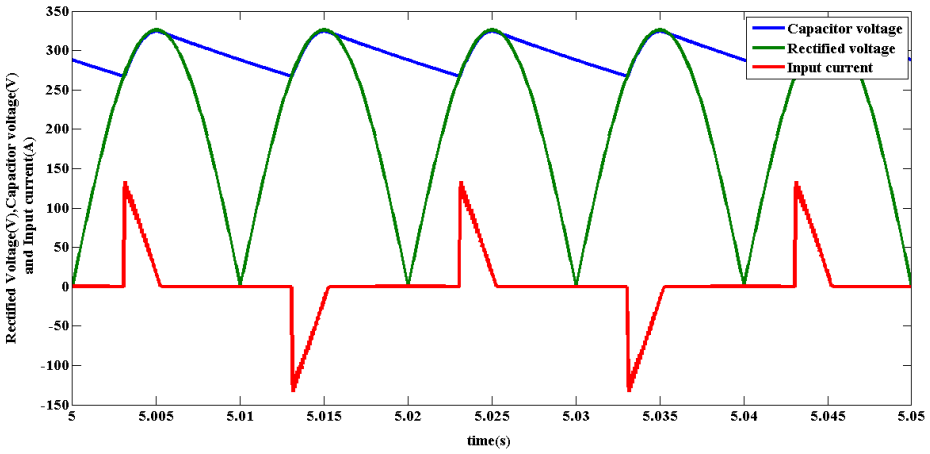

(b)

Fig 2.3 Diode rectifier with C filter (a) input current FFT analysis (b) rectified voltage capacitor voltage and input current (input current is magnified by ten times for better visibility)

Fig 2.3(b) shows the steady state capacitor voltage and input current waveform. The rectified voltage without any filter is shown in green color. When the input voltage or rectified voltage less than the voltage across capacitor the diodes are reverse biased and no current flows into the converter and the load current is supplied by the capacitor. When the supply voltage more than the capacitor voltage the diodes become forward bias and the capacitor draw charging current from the supply for a short duration. When the supply voltage is less than the capacitor voltage simultaneously the four diodes, get reverse biased. If the capacitor tends to infinity, the input current is an impulse current only. The power factor of the converter is 0.657, and the THD is 144.5% which exceeds the standards.

2.4.2 With LC filter

With LC filter, the rectifier operates in two modes i.e. CCM and DCM. When the inductor is very large as compared to the capacitor, the rectifier operates in CCM. The large inductor does not allow a sudden change in current and hence the inductor current is constant. The constant inductor current is supplied by the input diode rectifier with at least two diodes conducting. The input current is in phase with the input voltage . Hence the displacement factor is unity. However, the shape of current is not sinusoidal hence by introduces THD. In Discontinuous Conduction Mode the inductance value is small as compared to the capacitor. Due to the presence of inductor the input current width increases and inductor smoothens the current.

Several LC branches can be connected as a filter, and harmonic trap filter can be implemented at the input side with a series branch of RLC. With the addition of inductor on the output side of the diode rectifier the THD and PF improves. The results are shown in Fig 2.4.

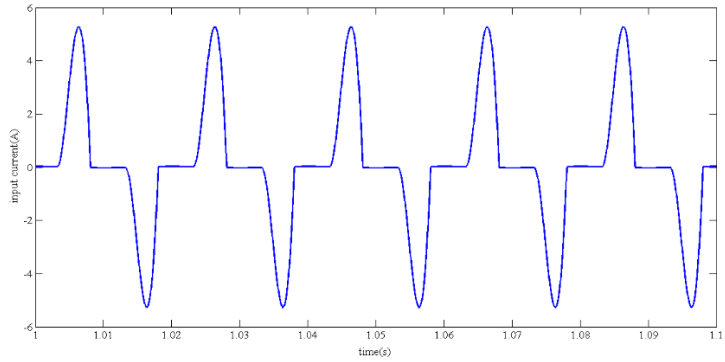

(a)

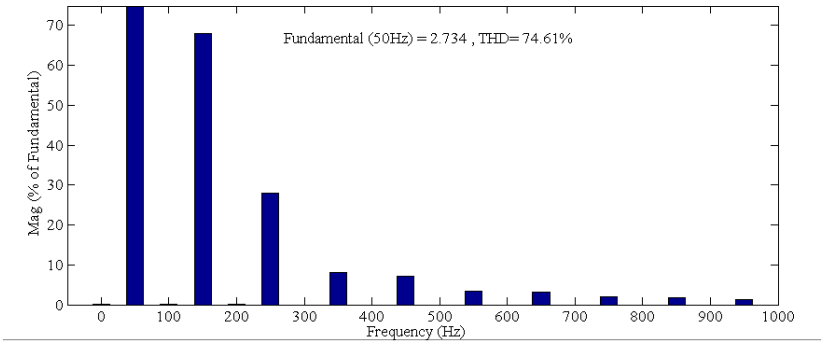

(b)

Fig 2.4 Diode rectifier with LC filter (a) input current (b) FFT of input current(L= 20 mF and C=200µF)

The THD reduces from 144 % to 74 % with the addition of filter inductance. With the increase in L value, the THD decreases and at the same instance the output voltage decreases and to maintain the desired output voltage another DC-DC converter with boost operation is necessary. The THD gets better with the harmonic trap filter at the input side. Fig 2.5 shows a graph between Inductance and THD. With infinite inductance, the pf cannot reach more than 0.9 [17].

Passive filters cannot make power factor more than 0.75 and only applicable for low power applications. Some disadvantages of passive filters are size, high THD, low pf,

unwanted resonance. Due to the disadvantages, active techniques are adopted at high power levels.

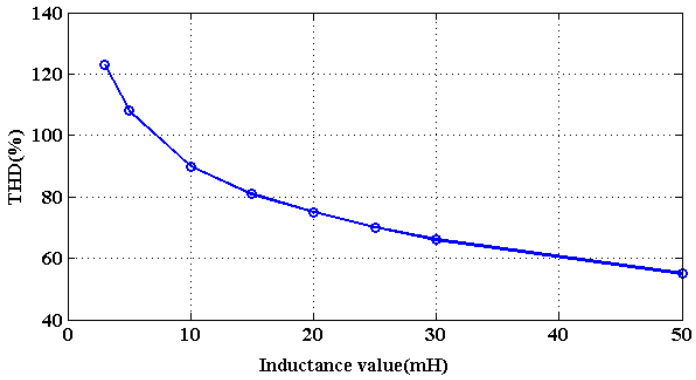

Fig 2.5 Filter inductance versus THD graph

2.5 Active PFC Converter

Due to various limitations of passive PFC techniques and to achieve unity power factor with very less THD active PFC techniques are implemented. Various switching converter topologies are used to force the input current to follow the shape of input voltage thus by reducing the harmonics and improving the PF. With the implementation of active PFC, the AC-DC converter behaves like a resistive load and draws sinusoidal input current. Active PFC devices produce less ripple voltage and the size of reactive elements much reduced because of high switching frequencies.

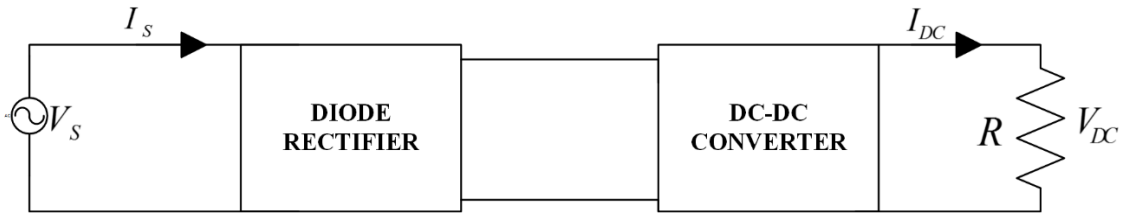

Fig 2.6 Block Diagram of Active PFC

The block diagram shows a basic AC-DC converter with power factor correction. The Diode rectifier is suitable only for unidirectional power flow i.e. Grid to Vehicle in the case of an On-Board EV charger. To achieve bi-directional power flow in G2V and V2G manner, the diode is replaced by IGBT or MOSFET and the rectifier can operate as an inverter in V2G mode of operation.

The DC-DC converter can be a Buck, Boost or Buck-Boost depending on the output voltage requirement. Buck converter produce an output voltage lower than input supply voltage whereas Boost converter produces a voltage higher than the supply voltage at the output terminals. The output voltage can be higher or lower than the supply voltage in the case of a Buck-Boost converter, but the component stress of Buck-boost converter is double to that of Buck or Boost topology hence it is not recommended. The DC-DC converter stage can be an isolated converter i.e. flyback or forward which can provide galvanic isolation between the Grid and EV. Depending on the operation of these converters in CCM or DCM the inductor current can be continuous or discontinuous. A discontinuous inductor current reaches zero in each switching cycle whereas a continuous inductor current never touches zero and have less ripple. Only in the case of Boost converter the input current is continuous and in Buck and Boost it is discontinuous because of the interruption of the switch in each switching cycle.

2.6 Boost PFC Converter

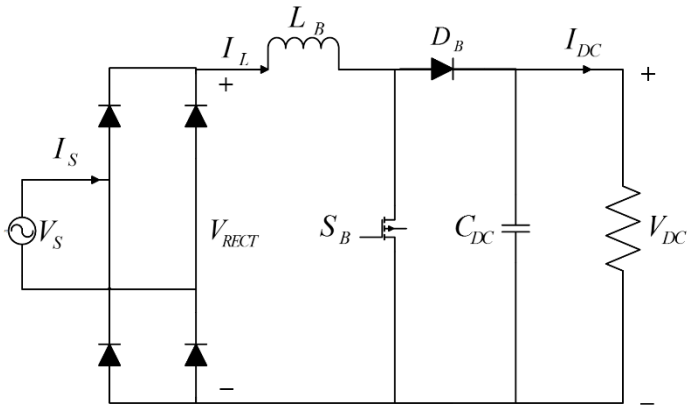

Fig 2.7 Boost PFC converter

Fig 2.7 shows a power stage circuit diagram of a Boost PFC converter. The input supply voltage is first rectified by a diode bridge rectifier and a Boost converter added at the later stage to make soppy current sinusoidal.

2.6.1 Switching operation of Boost converter

The line voltage is converted into a rectified DC voltage via Diode rectifier before the Boost converter. The input voltage to the Boost converter is the rectified voltage which varying from zero to peak value of the supply voltage. The pulsating input DC voltage can

be assumed as a constant DC voltage source for the analysis and operation of the Boost converter purpose. The Boost converter circuit configuration with both ON and OFF interval equivalent circuits are shown in Fig 2.8.

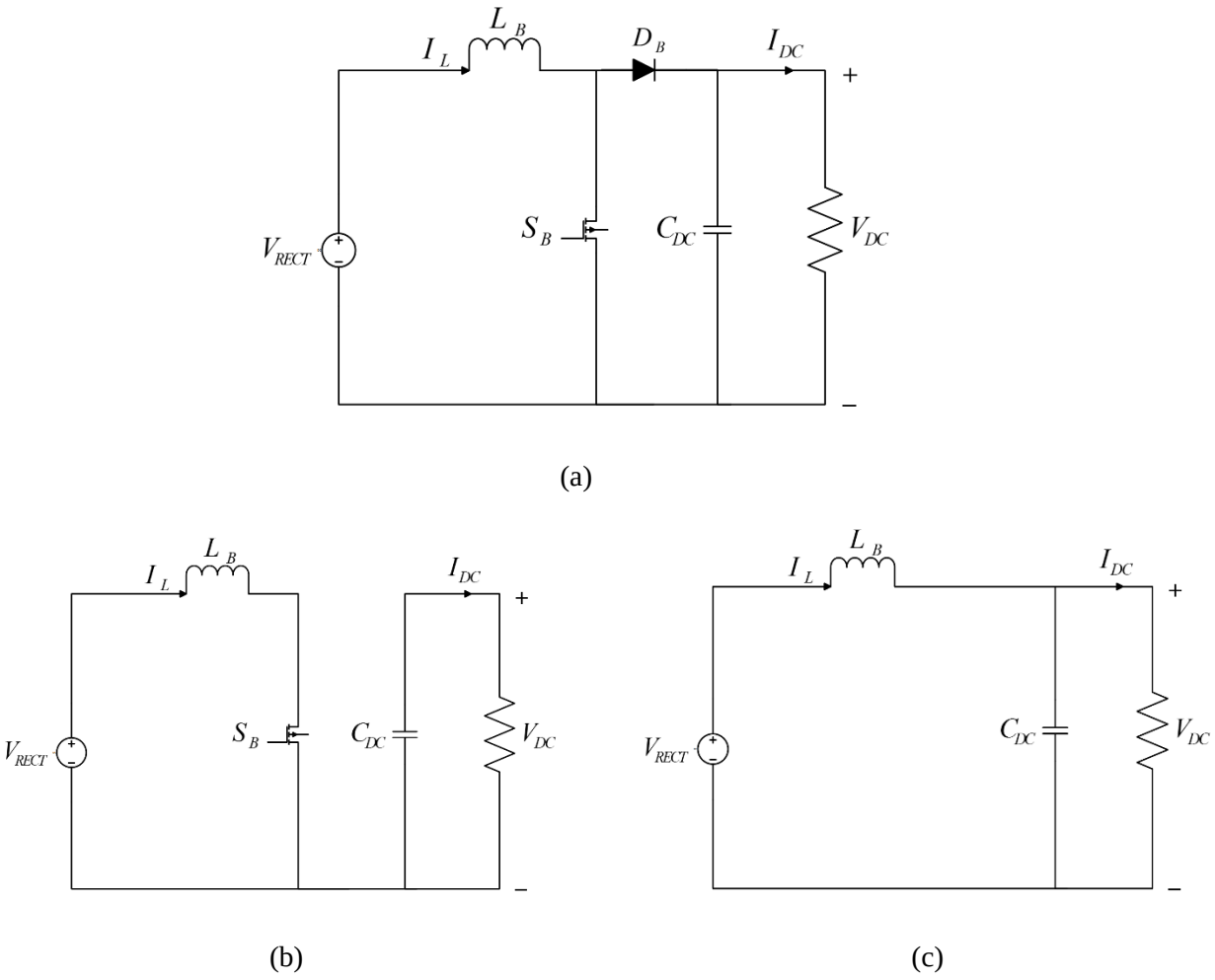

Fig 2.8 (a) Boost converter and equivalent circuit during (b) ON interval (c) OFF interval

Fig 2.8 describes the ON and OFF interval circuit model of Boost converter. During the time interval, $0 \le t \le DT_s$ the Boost switch S_B is turned ON by gate pulse, where D is the duty cycle and T_s is the switching period which is reciprocal of switching frequency. At this interval, the boost inductor L_B gets short-circuited via switch and input voltage V_{RECT} .The boost diode is reverse biased, and the load is supplied by the DC link capacitor. The inductor current i_L and capacitor voltage v_C can be described by

$$\frac{di_L}{dt} = \frac{V_{RECT}}{L} \tag{2.8}$$

$$\frac{dv_C}{dt} = -I_{DC} = \frac{V_{DC}}{R} \tag{2.9}$$

During the interval, $DT_s \le t \le T_s$ the switch is turned OFF while the boost diode is forward biased. The load is connected across the supply via the inductor. The OFF stage of the circuit is shown in Fig 2.8I. The dynamic equations of the inductor current and capacitor current can be written as

$$\frac{di_L}{dt} = \frac{1}{L}\left(V_{RECT} - V_{DC}\right) \tag{2.10}$$

$$\frac{dv_C}{dt} = i_L - I_{DC} \tag{2.11}$$

Both modes are repeated for every switching cycles.

2.6.2 Different modes of operation

Depending on the inductor current waveform boost converter operation is classified into three types i.e. Continuous Conduction Mode (CCM), Discontinuous Conduction Mode (DCM) and Critical Conduction Mode (CrCM) or Boundary Conduction Mode (BCM).

In CCM, the inductor current never reaches to zero. From Eq. 2.8 and 2.10 it can be observed that the inductor current increases during ON time and decreases during OFF time.During OFF time, there is a possibility of DCM if the inductor current reaches to zero. The advantages of CCM is the higher efficiency of the converter and low current stress on components. However, the disadvantage is a separate current controller is necessary for input current shaping so that the input current will follow the input voltage.

In DCM, the inductor current goes to zero in OFF interval if each switching cycle. The voltage and current stress on power devices are more in DCM but DCM has an advantage of inherited wave shaping of the input current. No separate current controller is required in case of DCM for input current shaping.

In BCM, the inductor current is just discontinuous.

The simulated inductor current waveform of both CCM and DCM mode are shown in Fig 2.9.The DCM provides a sinusoidal input current whereas the input current in case of CCM is non-sinusoidal and needs a further current controller. For CCM operation, the boost

inductance is taken as one mH whereas for DCM operation the inductance is chosen as 20μH.

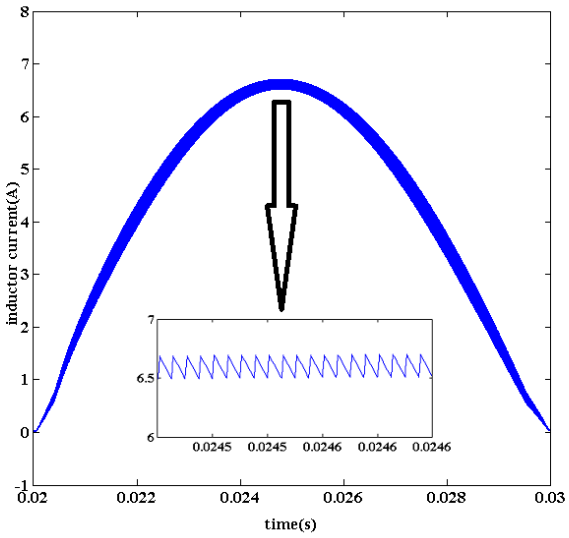

(a)

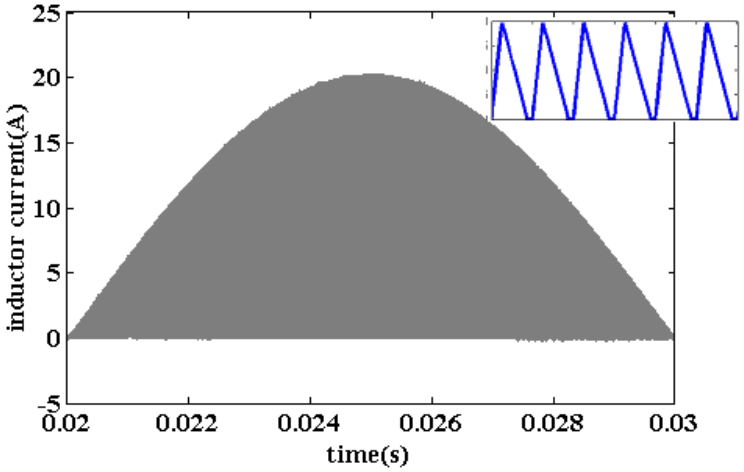

(b)

Fig 2.9 Inductor current in (a) CCM (b) DCM

2.6.3 CCM Boost PFC Converter Design

To achieve CCM of operation with the regulated output voltage and a sinusoidal input current, the parameters of the Boost PFC converter are designed on the basis of the specification listed in Table 2.3. According to the input and output specifications, various

components of Boost PFC converter are designed. The guidelines for designing is described in [18][19].

Table 2.3 AC-DC PFC converter specifications

Parameter	**Value**
Output Power	P_O=1000 W
Nominal output voltage	V_{DC}=450 V
Supply voltage	V_S=230 V (rms)
Supply frequency	f =50 Hz
Switching frequency	f_{sw}=200 kHz
Hold up time	t_h=20 ms

Considering the efficiency of the power stage is more than 95%.So $\eta_{max} \geq 95$ %.

Maximum input power at lowest efficiency can be calculated as:

$$P_{in(max)} = \frac{P_{O(max)}}{\eta_{max}} = \frac{1000}{0.95} = 1053\ W \tag{2.12}$$

The maximum and minimum input voltage can be assumed as 250 V and 210 V respectively.

The maximum input RMS and peak current can be calculated by taking minimum value of input voltage.

$$I_{S(rms)max} = \frac{P_{in(max)}}{V_{S(rms)min}} = \frac{1053}{210} = 5.01\ A \tag{2.13}$$

$$I_{S(peak)max} = \sqrt{2} \times I_{S(rms)max} = 7.1\ A \tag{2.14}$$

Boost inductor can be calculated by taking the inductor current ripple. Here the ripple current is taken as 10 % of the peak input current.

$$\Delta i_l = 0.1 \times I_{S(peak)max} = 0.71\ A \tag{2.15}$$

Where Δi_l is the inductor ripple current.

Maximum Duty cycle of the converter can be calculated as:

$$D_{max} = 1 - \frac{V_{S(peak)min}}{V_O} = 0.34 \tag{2.16}$$

Minimum value of inductor to satisfy the ripple current requirement is

$$L_{B(min)} = \frac{V_{S(peak)min} \times D_{peak}}{f_{sw} \times \Delta i_l} = 711.1\mu H \tag{2.17}$$

Output capacitor must satisfy the allowable output voltage ripple $\Delta v_{DC} = 10\ V$ peak-peak.

$$C_{DC} \geq \frac{P_O}{2\pi \times f \times \Delta v_{dc} \times V_{DC}} \tag{2.18}$$

And $C_{DC} \geq \frac{2 \times P_O \times t_h}{V_{DC}^2 - V_{DC(min)}^2}$ (2.19)

C_{DC} is calculated as $700\mu F$.

2.7 Controller Design

The power stage diagram of the Boost PFC converter is shown in Fig 2.7.The circuit consists of a diode bridge rectifier followed by a Boost converter for power factor correction. Switch S_B can be controlled in a close loop manner to maintain a desired voltage across the DC link capacitor and a sinusoidal input current. One common control method of PFC converters is Average Current Mode(ACM) Control [20][21].

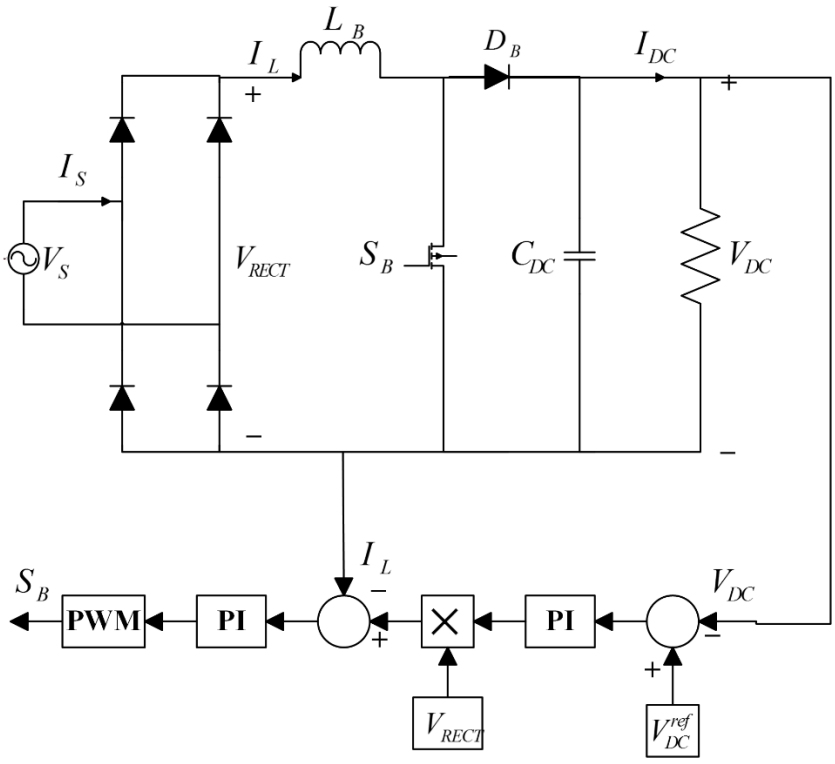

Fig 2.10 Boost PFC converter with ACM controller

The block diagram of a controller with the converter is shown in Fig 2.10. The controller consists of two loops. The outer loop is voltage loop to maintain the desired voltage at output terminals and the inner current loop controls the shape of the input current and enables the input current to follow the shape of the input voltage. The switching frequency of the converter is much higher than the supply frequency. In the case of the designed converter, the supply frequency is 50 Hz where the switching frequency is 200 kHz. The inner current loop is much faster than the outer voltage loop. Usually, the current loop bandwidth is in between one fifth and one tenth of switching frequency while the voltage loop bandwidth is around one-tenth of the bandwidth of the current loop or one-fifth of supply frequency. The voltage controller compares the desired DC link voltage with the actual one and generates an output depending on the error voltage. The error voltage multiplied with a reference sinusoidal shape to generate a reference current. The obtained reference current compared with the actual rectified current and given to the current controller. The controller produces an output in order to track the reference current. The amplitude of the reference current is decided by the output of voltage controller.

The output of voltage error amplifier is multiplied with the sensed DC output voltage of diode bridge rectifier V_{RECT} which is a rectified sinusoidal wave to generate a sinusoidal reference current. The reference current I^{ref} is compared with actual inductor current I_L .Depending on the error in the current the current controller produces a control signal which is compared with a sawtooth wave to produce gate pulse for the switch S_B .The frequency of the sawtooth carrier is same as designed switching frequency of the converter.

2.7.1 Current Controller

As described above the current loop is a fast loop with a bandwidth of in-between one tenth to one fifth of switching frequency. The inductor current is sensed by a current sensor and compared with the reference current that is generated by voltage error amplifier.

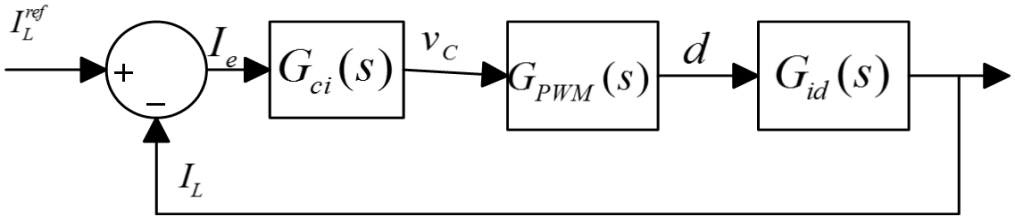

Fig 2.11 Current loop block diagram

Fig 2.11 shows the current loop of the PFC converter. While designing the current loop the voltage controller is assumed to be unity and the reference current is perfectly sinusoidal. $G_{id}(s)$ is the control-to-inductor current transfer function of the converter. $G_{PWM}(s)$ is the transfer function of the PWM generator and the value is $\frac{1}{V_{pwm(p-p)}}$, where $V_{pwm(p-p)}$ is the peak-to-peak voltage of sawtooth carrier. $G_{ci}(s)$ is the current controller.

By considering the saw-tooth carrier peak-to-peak voltage equals to one volt, the high frequency approximated open loop transfer function of the converter is

$$G_{id}(s) = \frac{V_{DC}}{sL_B} \tag{2.20}$$

The current controller is a PI type controller, and the transfer function can be written as

$$G_{ci}(s) = k_{pi} + \frac{k_{vi}}{s} \tag{2.21}$$

Where, k_{pi} and k_{vi} are the proportional and integral values.

The bandwidth is chosen as 30 kHz, and the controller is designed according to with frequency response analysis. The Bode plot of the converter in open loop and closed loop is shown in Fig 2.12.The phase margin is found to 49 degrees with a bandwidth of 26.5 kHz which is desired for current loop design.

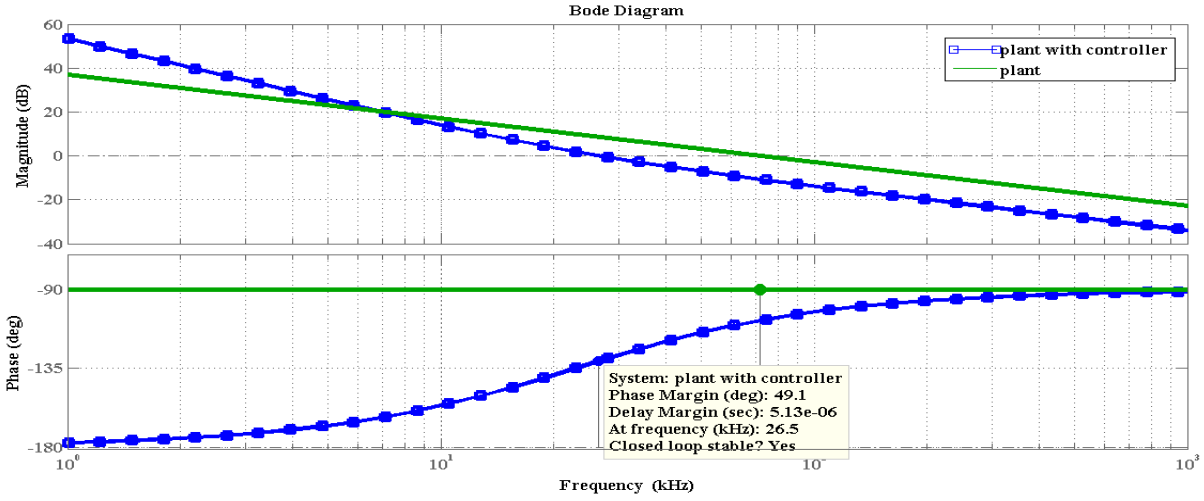

Fig 2.12 Bode plot of plant and plant with current controller

2.7.2 Voltage Controller

The design of voltage controller is similar to the current controller, but the bandwidth is chosen as less than line frequency i.e. around 20 Hz. Due to very low bandwidth, the voltage loop is very slow in operation. The feedback voltage is sensed across the load and then passed through a low-pass filter in order to suppress high-frequency components of the output voltage. The error voltage is generated after comparison of the output voltage with the desired and fed to the voltage error amplifier. The voltage error amplifier is a PI type controller with low BW to suppress the ripple in the error voltage. The voltage controller is designed by following PI controller designed procedure, and the total controller is implemented in the PFC converter to get desired results which are shown in section 2.8.

The controller does not have any information about the input voltage, so with the variation of the input voltage, the response of the controller does not change. To make the controller dependent on the input voltage, a voltage feedforward block is added to the controller in conventional PFC controllers. However, implementation of voltage feed forward is more challenging. A new approach to design the controller to track the input voltage is by adjusting the gain of the reference current depending on the RMS value of the input voltage.

2.8 Simulation and Results

The CCM Boost PFC converter described above is simulated using MATLAB/27Simulink with Peak Current Mode control, and some of the simulated results are shown below.

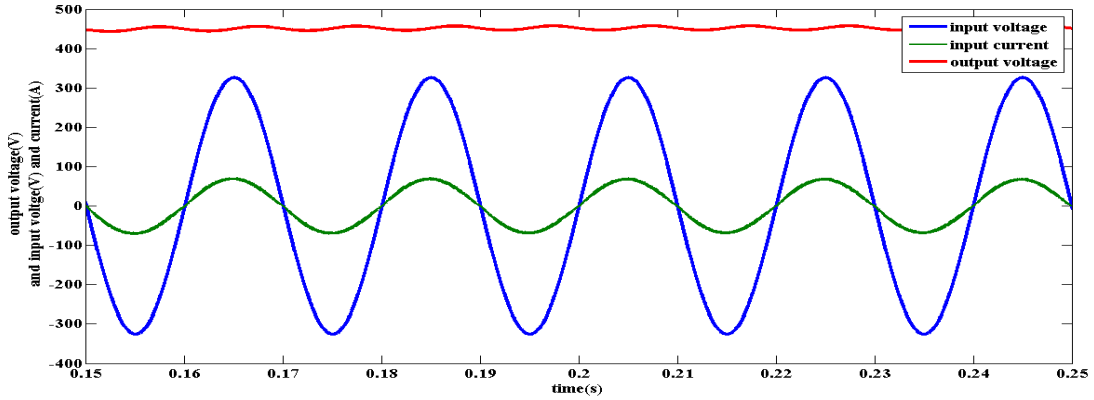

(a)

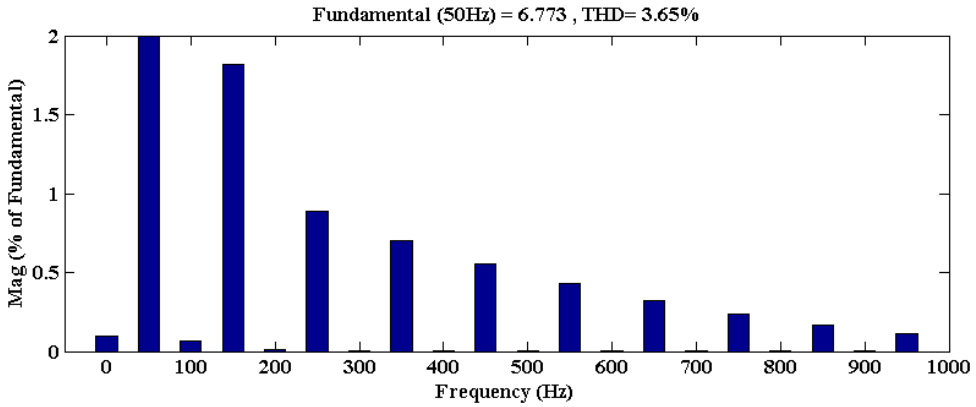

(b)

Fig 2.13 Boost PFC results for 1000 W load (a) input voltage and current (scaled ten times) and output voltage, (b) THD of input current($L_B = 1mF, C_{DC} = 700\ \mu F, f_{sw} = 200kHz, V_s = 230\ V\ rms$)

As it can be noted from the waveforms in Fig 2.13 (a), the nominal output voltage is 450 V with a ripple of 10 V peak-to-peak and the RMS current is 4.9 A and follows the input voltage waveform. The input current is enlarged ten times for better visibility. The THD is found to be 3.65 % as shown in the FFT analysis of input current in Fig 2.13(b) and using Eq. 2.7 the pf is calculated as 0.9993.The THD of the designed converter is very less than a conventional diode rectifier, and the THD satisfies the IEEE standard of harmonics.

As explained before the output stage of an AC-DC converter is usually a DC-DC converter with constant power application. However if the power decreases the converter operates satisfactorily with desired output voltage and an increased value of current harmonic. The output voltage, input voltage and current and the FFT of the input voltage of the designed converter at half load are shown in Fig 2.14.The THD is found to be 5 % with a pf of 0.9987.

Various simulations are performed with varying the load power and input voltage in order to get the desired voltage across the DC link and THD below the prescribed standards.

The load power varies between a range of 760 W to 1000 W when the battery charging from beginning point to turning point with maximum power at turning point. The designed PFC converter produces a THD less than 5 % over the wide range of variation of load power i.e. 760 W to 1000 W.

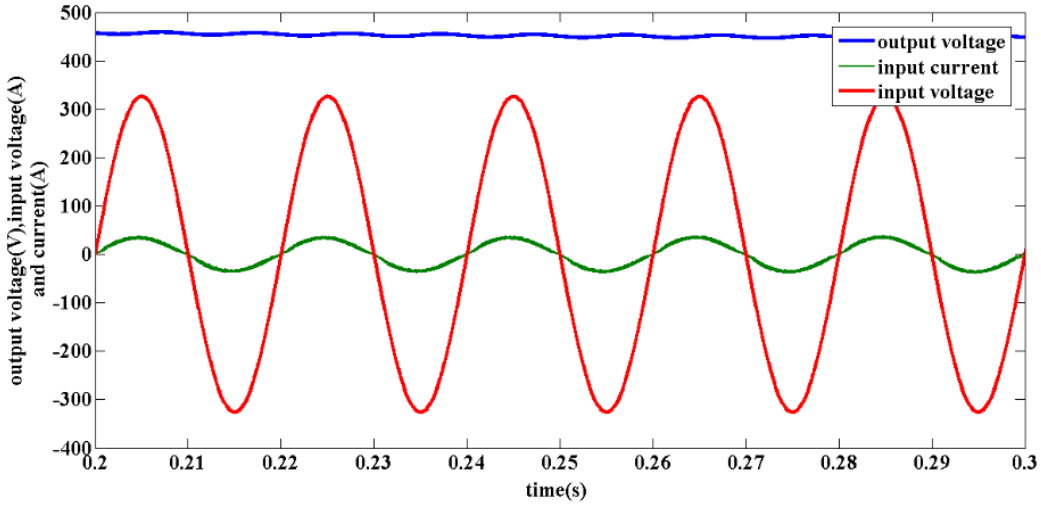

Fig 2.14 Boost PFC converter operating at Half-Load output voltage, input voltage and current(scaled ten times for better visibility) of Boost PFC converter operating at Half-Load

$(L_B = 1mF, C_{DC} = 700\ \mu F, f_{sw} = 200kHz, V_s = 230\ V\ rms)$

Fig 2.15 shows the input and output current waveform when the load changes from 500 W to 1000 W. The transient period stays for 5-7 line cycles then the voltage and current stabilizes after 7 line cycles i.e. 140 ms.The output and input currents are 1.11 A and 2.48 A (RMS) when the load is 500 W and the input current chnages to 4.95 A (RMS) when the load changes to 1000 W and the output current also doubles after the load change.

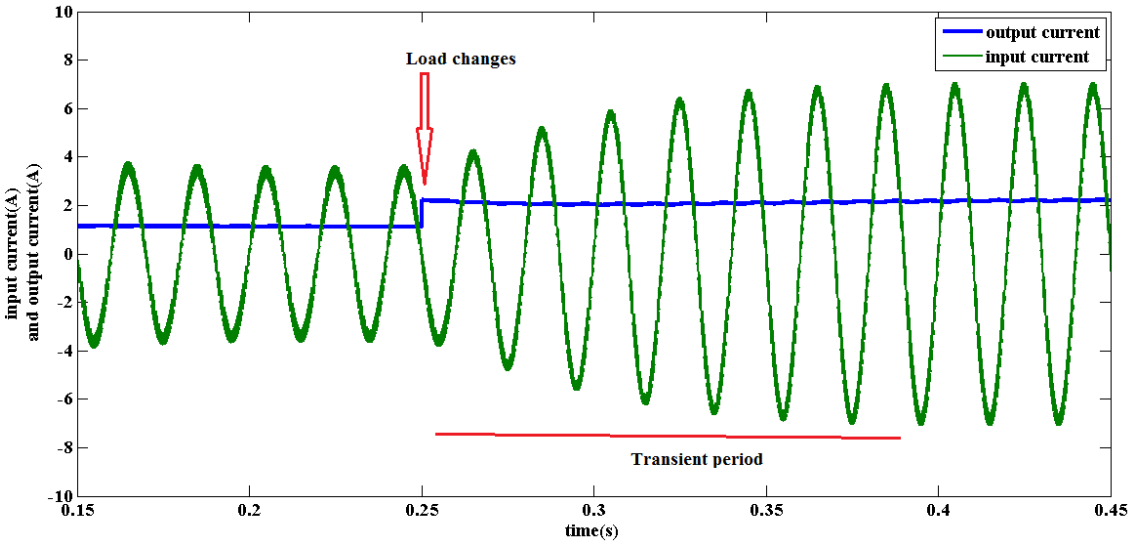

Fig 2.15 Input current and output current when a step load changes from 500 W to 1000 W.

$(L_B = 1mF, C_{DC} = 700\ \mu F, f_{sw} = 200kHz, V_s = 230\ V\ rms)$

2.9 Conclusion

In this chapter, the basic definitions and calculations of power factor and total harmonic distortion are explained. The important disadvantages of commonly used diode rectifier are stated, and the solution of THD is resolved using active PFC converters. A CCM Boost PFC converter is designed and simulated calculated parameters in section 2.6.3.The ACM controller is designed with a high bandwidth inner loop current controller and a slow speed voltage controller. The input current is observed to be perfectly sinusoidal with very less harmonics under full load condition. However with any variations of output power or input voltage the THD gets affected so as the pf. With the decrease in load power the THD increases. The PFC converter usually followed by a resistive load or a DC-DC converter which operates with a constant power. But, in the case of OBC, the PFC converter is followed by a DC-DC converter demanding variable power depending on the state of charge of battery. The DC-DC converter's output power varies widely in between 760 W to 1000 W and in this range of operation, the designed PFC converter maintains preferred DC link voltage with low THD that satisfies the standards provided in Table 2.2 and 2.3. The bidirectional DC-DC converter followed by Boost PFC converter to control the battery voltage and current is described in next chapter.

CHAPTER 3

BACK-END DC-DC CONVERTER

3.1 Introduction

The charging profile of a Li-ion cell is explained in 1.3.The EV battery bank is usually a series-parallel combination of Li-ion cells to increase energy by increasing the voltage and current rating. To charge the high voltage battery in CC/CV modes, a second stage DC-DC converter is implemented on OBC. As described in the previous chapter 2 the output voltage of the front end AC-DC PFC converter is 450 V DC with a ripple voltage of 10 V peak-to-peak. The nominal voltage of the battery is 360 V from depleted condition 320 V to fully charged condition 420 V. A second stage converter is desired which can operate with an oscillating input voltage that is produced by the first stage AC-DC converter and can produce a wide range of output voltage. A DC-DC converter is adopted for the necessary operation.

The surplus amount of energy of the EV battery can be supplied to the Grid when connected in V2G manner. To support power flow in a reverse direction the second stage DC-DC converter should be capable of bidirectional power flow.V2G operation is not the objective of an OBC as the vehicle battery energy is very less as compared to the Grid. However in the case of emergency, the battery energy can be utilized to run home appliances by allowing the power flow through DC-DC converter in a reverse manner.

Addition to the high voltage battery pack another low-voltage auxiliary battery is present in EV or HEV. Auxiliary battery is a low voltage battery (12 V) utilized to supply power to the electronic loads of the vehicles such as lights music system etc. Conventionally alternators are employed to charge the auxiliary battery while driving in IC engine vehicles even in EVs. The losses associated with charging the auxiliary battery via the alternator is relatively more as the electrical energy is converted into mechanical and again into electrical and require additional power converters. In order to minimize the losses, the OBC is modified to work as a Low-Voltage DC-DC Converter (LDC) by supplying the power from propulsion battery into auxiliary battery in driving stage [25].

Advantages of Bi-Directional DC-DC converter in Battery charging operation:

- Both G2V and V2G mode of power flow
- Maximum efficiency and minimum circuit complexity.
- Desired CC/CV mode of control with wide output voltage range.
- Less ripple in charging mode.
- Suitable for charging the auxiliary battery via the propulsion battery.

Bidirectional DC-DC converter classification:

The major purpose of the bidirectional converter is to control power flow in both directions. Many topologies are available with bi-directional power flow capability. One major reason for classifying the bidirectional DC-DC converter is the presence of Isolation. An isolation transformer provides galvanic isolation between the two voltage levels of the converter [21]. Depending on the isolation the converter is classified into two categories

- Non-isolated Bidirectional DC-DC converter
- Isolated Bidirectional DC-DC converter

The operation of Non-Isolated Bidirectional Converter is explained in this research work. The controller is designed with CC/CV mode operation for the same.

3.2 Non-Isolated Bidirectional DC-DC Converter

Conventional DC-DC topologies such as Buck and Boost converters support only unidirectional operation. In order to achieve G2V and V2G modes of operation two converters are required for each operation which will increase the components and circuit complexity. The traditional unidirectional converters can be modified to bidirectional with a minute change in circuit configuration and by replacing the diodes into MOSFETs or IGBTs.

3.2.1 Bidirectional Half-Bridge DC-DC Converter

A Half-Bridge Converter is a Buck-Boost derived converter where both converters connected antiparallel that supports bidirectional power flow [22, 23]. The circuit diagram is shown in Fig.3.1, and the operation of both forward and reverse directions are discussed below.

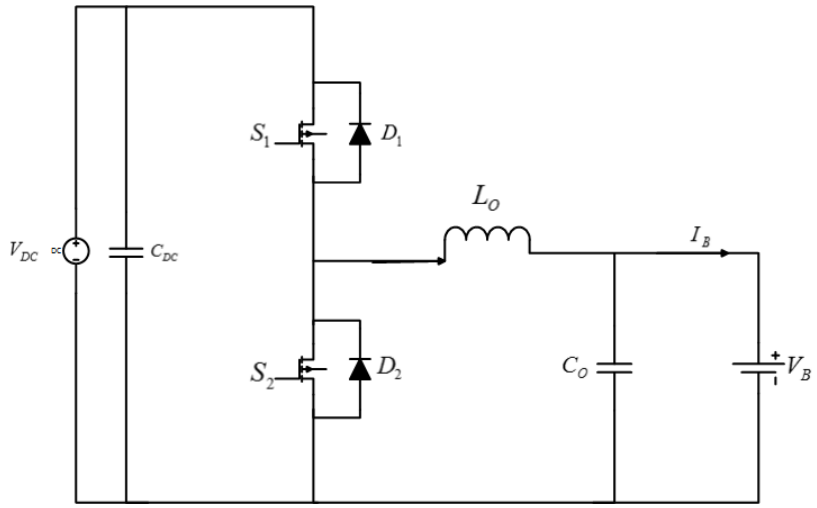

Fig 3.1 Non-isolated Half-Bridge DC-DC Converter

Where,

V_{DC}: DC link Voltage

L_O: Filter Inductance

C_O: Filter Capacitance

V_B: Propulsion Battery

I_B: Battery current

The above topology operates both in Buck mode and Boost mode depending on the operation of switched S_1 and S_2. D_1 and D_2 are antiparallel diodes with the switches and behave as freewheeling diodes. As the DC link voltage is about 450 V and the battery voltage varies 320-420 V the converter operates as a buck converter during charging the battery from the grid and during V2G operation it boost the battery voltage to 450 V by operating as Boost converter. A brief explanation of the above converter is presented below.

3.2.1.1 G2V Mode

In this mode, the converter operates as a Buck converter i.e. output voltage is less than the input. Switch $S_1$and diode D_2 conduct while S_2 and D_2 remains OFF during complete cycle as shown in Fig 3.2.

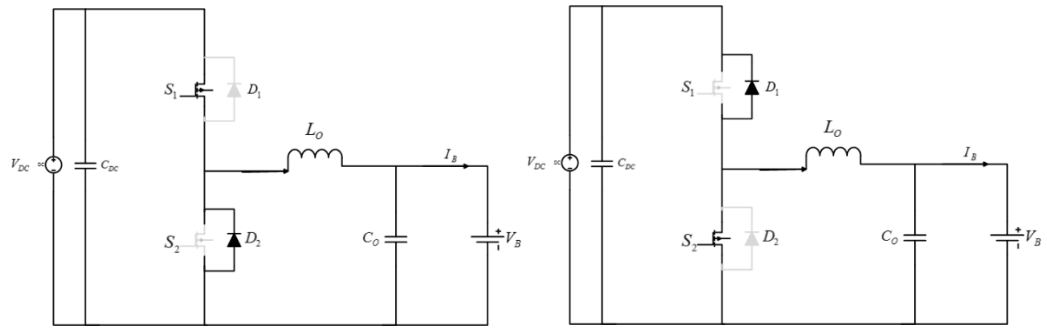

(a) (b)

Fig 3.2 Half-Bridge DC-DC Converter (a) G2V mode (b) V2G mode

When S_1 is turned ON the battery V_B is connected to the DC link through filter inductor L_O and the inductor stores energy. Inductor current increases in with a slope of $\frac{V_{DC}-V_O}{L_O}$ and stores energy. The load current is the difference of inductor current and capacitor current. After S_1 turned OFF the inductor releases the energy via forward biasing the diode D_2.The current decreases linearly. Load current remains at steady state value as the high frequency components of inductor ripple current bypassed through the filter capacitor. Both ON and OFF intervals are shown in Fig 3.3.

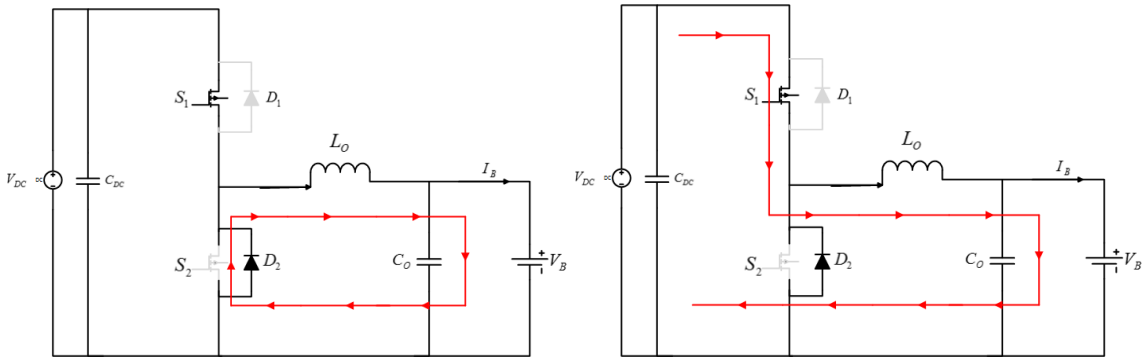

(a) (b)

Fig 3.3 G2V operation (a) ON interval (b) OFF interval

The equations for output voltage, ripple current, and ripple voltage are same as conventional Buck converter [24].

$$V_B = D \times V_{DC} \tag{3.1}$$

$$\Delta I_L = \frac{D(1-D)V_{DC}}{f \times L_O} \tag{3.2}$$

$$\Delta V_B = \frac{D(1-D)V_{DC}}{8 \times f^2 \times L_O \times C_O} \tag{3.3}$$

Where,

ΔI_L: Ripple in battery current

ΔV_B: Ripple in battery voltage

D: Converter duty cycle

f: switching frequency

3.2.1.2 V2G Mode

In V2G mode, the converter acts as a Boost converter by stepping up the battery voltage into DC link voltage 450 V for further application. Here switch S_2 and diode D_1 conducts depending on the duty ratio while S_1 and D_2 remains OFF during complete cycle.

When S_2 is gated the battery gets short circuited through the inductor L_O and the inductor stores charge. In the second mode when the switch S_2 turned OFF the stored charge in the inductor forward bias the diode D_1 and the battery is connected to V_{DC} via the inductor L_O.The expression forV_{DC}, L_O and C_{DC} are similar as conventional Boost converter.

$$V_{DC} = \frac{V_B}{1-D} \tag{3.4}$$

The above converter can operate as a synchronous Buck converter in G2V mode and synchronous Boost converter in V2G application and that can be done by operation both switches S_1 and S_2 in a complementary manner. For example in G2V mode the converter works as Buck converter. During ON interval switch S_1 is triggered with a positive gate pulse while its complementary gate pulse is given to S_2 and S_2 remains in OFF condition. During OFF condition the positive gate signal withdrawn from S_1 where as S_2 is turned ON due the complementary gate signal which is a positive pulse. As both switched as turned ON or OFF with a single gate pulse in a synchronous manner the converter is named as synchronous DC-DC converter. In this work the DC-DC converter operates in a synchronous manner.

3.4 State Space Averaging

A system can be described by various linear and non-linear equations. In state space averaging the converter is expressed by the differential equations. The converter can be an ideal one or a practical including the parasitic resistances of inductor and capacitors with

switch resistances. The number of reactive elements associated with the converter provides the state variables X (t).In this discussion, the state space model of Buck and Boost converter is derived.

The generalized state space equations are

$$\frac{dX(t)}{dX} = A.X(t) + B.U(t) \tag{3.5}$$

$$Y(t) = C.X(t) + E.U(t) \tag{3.6}$$

Where X (t): state matrix

U(t): input matrix

Y(t): output matrix

The state equations can be written for both ON and OFF intervals.

During ON interval, the converter can be expressed as

$$\frac{dX(t)}{dt} = A_{ON} \times X(t) + B_{ON} \times U(t) \tag{3.7}$$

$$Y(t) = C_{ON} \times X(t) + E_{ON} \times U(t) \tag{3.8}$$

Similarly during OFF interval the converter can be stated as

$$\frac{dX(t)}{dt} = A_{OFF} \times X(t) + B_{OFF} \times U(t) \tag{3.9}$$

$$Y(t) = C_{OFF} \times X(t) + E_{OFF} \times U(t) \tag{3.10}$$

At equilibrium state of the converter

$$0 = A.X + B.U \tag{3.11}$$

$$Y = C.X + D.U \tag{3.12}$$

Where A, B, C, D are averaged matrices and are expressed as

$$A = DA_{ON} + D'A_{OFF} \tag{3.13}$$

$$B = DB_{ON} + D'B_{OFF} \tag{3.14}$$

$$C = DC_{ON} + D'C_{OFF} \tag{3.15}$$

$$E = DE_{ON} + D'E_{OFF} \tag{3.16}$$

The state and output vector can be derived by solving the above equations. The state and output vectors are

$$X = -A^{-1}BU \tag{3.17}$$

$$Y = (-CA^{-1}B + E)U \tag{3.18}$$

3.4.1 G2V Mode

In G2V mode, the converter operation is similar as a Buck converter. The small signal modeling of a synchronous buck converter is derived here. The battery is modeled as its equivalent resistance for simplicity.

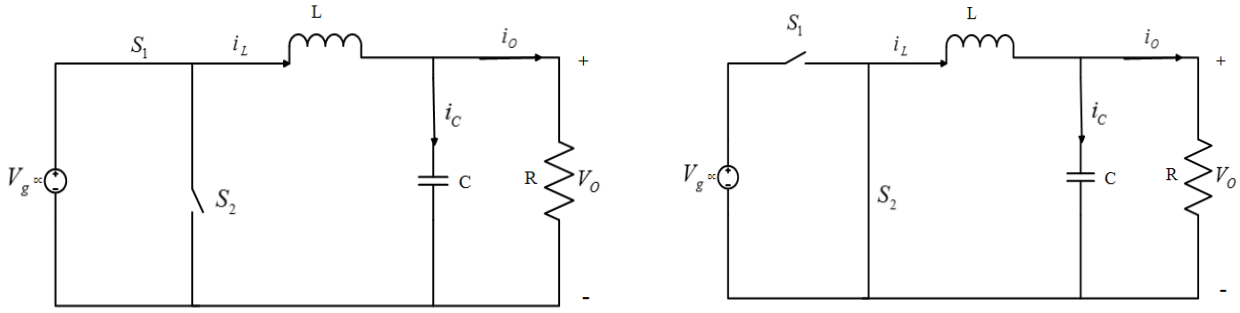

(a) (b)

Fig 3.4 Buck Converter (a) ON interval (b) OFF interval

Fig 3.4 shows the ON and OFF interval circuit of the synchronous Buck converter. L and C are the filter inductance, and capacitance is the equivalent battery resistance.V_g *and* V_O are input and battery voltage respectively. The parasitic resistances are neglected and the converter is assumed to be ideal. The state equations are derived as follows.

As explained in 3.2 when S_1 is ON and S_2 is OFF the load is connected to the input voltage via inductor.

$$V_g = L\frac{di_L}{dt} + v_C \tag{3.19}$$

$$\frac{di_L}{dt} = -\frac{1}{L}v_C + \frac{1}{L}V_g \tag{3.20}$$

The capacitor current is the difference of inductor current and load current.

$$i_C = i_L - i_O \tag{3.21}$$

$$\frac{dv_C}{dt} = \frac{1}{C} i_L - \frac{1}{RC} v_C \tag{3.22}$$

The output voltage $V_O = v_C$

Rearranging Eq. (3.7) and (3.8) into state space form

$$\begin{bmatrix} \frac{di_L}{dt} \\ \frac{dv_C}{dt} \end{bmatrix} = \begin{bmatrix} 0 & \frac{-1}{L} \\ \frac{1}{C} & \frac{-1}{RC} \end{bmatrix} \begin{bmatrix} i_L \\ v_C \end{bmatrix} + \begin{bmatrix} \frac{1}{L} \\ 0 \end{bmatrix} V_g \tag{3.23}$$

$$\begin{bmatrix} V_O \\ i_g \end{bmatrix} = \begin{bmatrix} 0 & 1 \\ 1 & 0 \end{bmatrix} \begin{bmatrix} i_L \\ v_C \end{bmatrix} + \begin{bmatrix} 0 \\ 0 \end{bmatrix} V_g \tag{3.24}$$

Renaming the matrices

$$A_{ON} = \begin{bmatrix} 0 & \frac{-1}{L} \\ \frac{1}{C} & \frac{-1}{RC} \end{bmatrix} \tag{3.25}$$

$$B_{ON} = \begin{bmatrix} \frac{1}{L} \\ 0 \end{bmatrix} \tag{3.26}$$

$$C_{ON} = \begin{bmatrix} 0 & 1 \\ 1 & 0 \end{bmatrix} \tag{3.27}$$

$$E_{ON} = \begin{bmatrix} 0 \\ 0 \end{bmatrix} \tag{3.28}$$

OFF Period:

When the switch S_1 is turned OFF and S_2 is turned ON the source is disconnected from the load and the stored inductor energy freewheels via load.

Appling KVL to the loop we get

$$v_L = -V_O \tag{3.29}$$

$$\frac{di_L}{dt} = -\frac{1}{L} v_C \tag{3.30}$$

The capacitor current is the difference of inductor and load current as in the previous condition.

$$\frac{dv_C}{dt} = \frac{1}{C} i_L - \frac{1}{RC} v_C \tag{3.31}$$

Rearranging Eq. (3.9) and (3.10) into state space form

$$\begin{bmatrix} \frac{di_L}{dt} \\ \frac{dv_C}{dt} \end{bmatrix} = \begin{bmatrix} 0 & \frac{-1}{L} \\ \frac{1}{C} & \frac{-1}{RC} \end{bmatrix} \begin{bmatrix} i_L \\ v_C \end{bmatrix} + \begin{bmatrix} 0 \\ 0 \end{bmatrix} V_g$$

(3.32)

$$\begin{bmatrix} V_O \\ i_g \end{bmatrix} = \begin{bmatrix} 0 & 1 \\ 0 & 0 \end{bmatrix} \begin{bmatrix} i_L \\ v_C \end{bmatrix} + \begin{bmatrix} 0 \\ 0 \end{bmatrix} V_g$$

(3.33)

Renaming the matrices

$$A_{OFF} = \begin{bmatrix} 0 & \frac{-1}{L} \\ \frac{1}{C} & \frac{-1}{RC} \end{bmatrix} \tag{3.34}$$

$$B_{OFF} = \begin{bmatrix} 0 \\ 0 \end{bmatrix} \tag{3.35}$$

$$C_{OFF} = \begin{bmatrix} 0 & 1 \\ 0 & 0 \end{bmatrix} \tag{3.36}$$

$$\boldsymbol{E}_{OFF} = \begin{bmatrix} \mathbf{O} \\ \mathbf{O} \end{bmatrix} \tag{3.37}$$

Linearization

The small signal model of the converter can be derived using perturbation around the steady state operating points (X, U,D).

$$x = X + x \tag{3.38}$$

$$u = U + u \tag{3.39}$$

$$d = D + d \tag{3.40}$$

x, u and d are small variations around the steady state values.

Substituting

$$\dot{x} = Ax + Bu + \left[\left(B_{ON} - B_{OFF} \right) U + \left(A_{ON} - A_{OFF} \right) X \right] d \tag{3.41}$$

$$y = Cx + Eu \tag{3.42}$$

Taking Laplace of the Eq.(3.41) and (3.42)

$$sx(s) = Ax(s) + Bu(s) + \left[\left(B_{ON} - B_{OFF} \right) U + \left(A_{ON} - A_{OFF} \right) X \right] d(s) \tag{3.43}$$

$$y(s) = Cx(s) + Eu(s) \tag{3.44}$$

Appling superposition theorem to Eq. (3.43) and (3.44)

$$x(s) = \left(SI - A \right)^{-1} Bu(s) + \left(SI - A \right)^{-1} \left[\left(B_{ON} - B_{OFF} \right) U + \left(A_{ON} - A_{OFF} \right) X \right] d(s) \tag{3.45}$$

$$y(s) = C\left[\left(SI - A \right)^{-1} Bu(s) + \left(SI - A \right)^{-1} \left[\left(B_{ON} - B_{OFF} \right) U + \left(A_{ON} - A_{OFF} \right) X \right] \right] d(s) + Eu(s) \tag{3.46}$$

Substituting the matrices the open loop transfer functions are obtained as

Control-to-output transfer function, $G_{v_o d}(s) = \dfrac{V_g R}{s^2 RLC + sL + R}$ (3.47)

Control-to-current transfer function, $G_{i_L d}(s) = \dfrac{V_g (1 + SRC)}{s^2 RLC + sL + R}$ (3.48)

3.4.2 V2G Mode

The transfer function of the converter in V2G mode can be derived using the above procedure. The converter works as a Boost Converter in V2G mode.

Control-to-output transfer function, $G_{v_o d}(s) = \dfrac{\left(V_g \big/ (1-D)^2 \right) \left((R(1-D)^2) - sL \right)}{s^2 LCR + SL + R(1-D)^2}$ (3.49)

Control-to-current transfer function, $G_{i_L d}(s) = \dfrac{V_g (2 + sCR)}{(1-D)\left(s^2 LCR + sL + R(1-D)^2 \right)}$ (3.50)

3.5 Design of Controller

The controller is divided into two categories. One is to regulate the battery voltage and current in G2V operation another is to control the power and voltage during V2G operation.

3.5.1 G2V operation

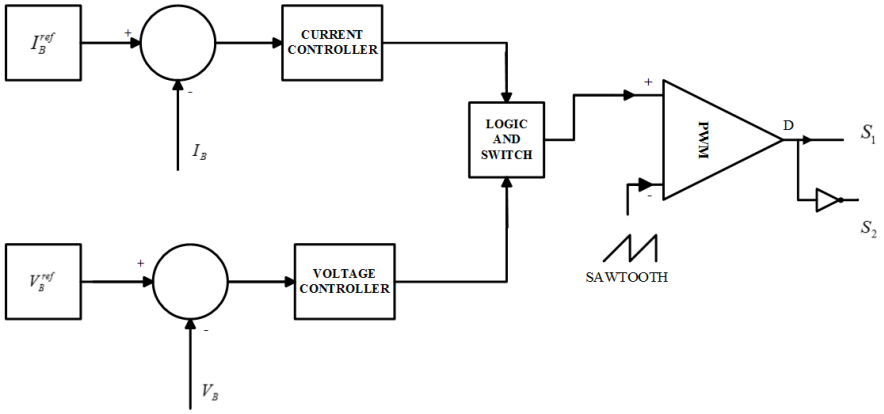

Fig 3.5 Controller for DC-DC converter in G2V operation

The objective of the controller is to regulate the charging process in CC/CV manner. The EV battery is charged in a CC mode up to the maximum voltage limit after than the CV mode is switched until the battery current limited to a predefined value. It is discussed formerly that the battery has a nominal voltage of 360 V with 420 V at fully charged and 320 V at the fully discharged condition. As shown in Fig 3.5 the controller consist of two control loops, first one is the current loop to regulate the battery current in CC mode and the second one is a voltage loop to monitor the battery voltage in CV mode.

A reference battery current is necessary for CC mode operation. The reference current can be chosen depending on the charging power level. For level 1 charging the reference current is considered as 2.38 A. The reference current is compared with the actual battery current and depending on the difference between the two an error signal is produced. The error is the input to the current controller and the output of the controller given to the PWM generator where the controller output is compared with a sawtooth signal having a frequency same as the desired switching frequency. The PWM generator produces the gate pulses for the switch S_1.Switch S_2 is triggered in a 180 degree phase difference manner.

The maximum battery voltage i.e. 420 V is the reference voltage for voltage controller. The battery voltage is compared with the reference voltage and given to the

voltage controller. Depending on the controller output the PWM generator provides gate pulses to both switches.

A logic and switching block is required for automatic switching between CC/CV modes depending on the battery voltage. The charging process starts with CC mode with minimum battery voltage 320 V(Beginning point).The battery voltage gradually increases keeping the battery current constant at the reference value. The logic unit continuously senses the battery voltage and when the voltage reaches maximum permissible voltage i.e. 420V (Turning point) CV mode is switched ON and the battery continues to charge in a constant voltage manner. The battery current gradually decreases while the voltage is constant. After reaching a predefined value the charging process stops (Endpoint).

3.5.1.1 Voltage Controller Design

As explained above the function of the voltage controller is to maintain a constant voltage across the battery in order to accomplish CV mode of charging. The voltage must remain constant in spite of any change in input DC link voltage or battery current variation. The controller continuously compares the battery voltage with the reference and generate duty ratio to maintain the desired voltage. The controller design is based on the control-to-output voltage transfer function in G2V mode.

From Eq. 3.47 the transfer function of the converter obtained as

$$G_{v_B d}(s) = \frac{V_{DC} R_B}{s^2 R_B L_O C_O + s L_O + R_B} \tag{3.51}$$

Putting the derived value of circuit elements the transfer function can be written as

$$G_{v_B d}(s) = \frac{450}{1.4\times10^{-10}\times s^2 + 3.98\times10^{-5} s + 1} \tag{3.52}$$

The phase margin and gain crossover frequency are 9° and 284 kHz respectively. A PI controller is required to boost the phase margin around 60° at a crossover frequency one tenth of switching frequency i.e. 20 kHz.

The transfer function of the PI controller is

$$G_{CV} = k_p + \frac{k_i}{s} \tag{3.53}$$

Where, k_p = proportional gain and k_i is integral gain.

The steps for designing the controller are as follows:

Desired Phase Margin (PM) = 60° at a crossover frequency of 20 kHz.

The uncompensated plant gain and phase at the desired crossover frequency are 39 dB and -104°. (From bode plot of the uncompensated plant)

Phase margin can be calculated as

$$PM = 180 + \angle G_P - 90 + \tan^{-1}\left(\frac{w_{gc}}{a}\right) \tag{3.54}$$

Where,

w_{gc} =cross over frequency in rad/s.

$\angle G_P$ =phase of the uncompensated system at w_{gc}.

$$a = k_i / k_p$$

The gain of compensated system at crossover frequency should be zero i.e. the sum of controller and plant gain has to be 0 dB at w_{gc}.

$$|G_P| + 20\log\left(k_p\sqrt{1+\left(\frac{a}{w_{gc}}\right)^2}\right) = 0dB \tag{3.55}$$

$|G_P|$ =gain of the uncompensated plant at w_{gc}.

On solving Eq. 3.55 The value of k_p and k_i are obtained.

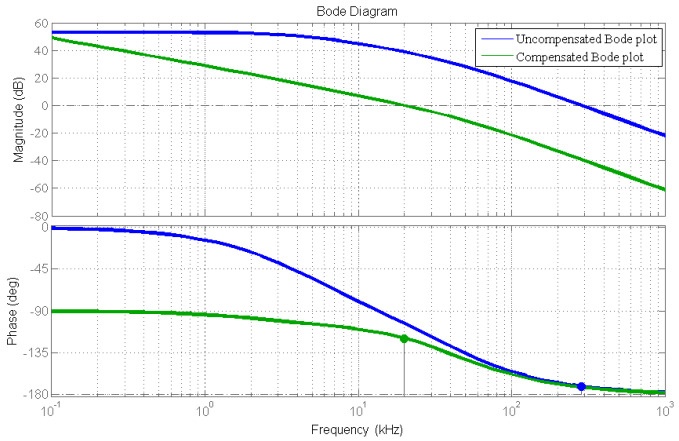

Fig 3.6 Bode plot of the plant with and without controller

Fig 3.6 shows the Bode plot of the system without a controller and with a controller. It can be observed that after adding the PI controller the phase margin is 60.5° at a frequency of 19.9 kHz as desired. After addition of the controller, the PM of the system improves hence by stability.

3.5.1.2 Current Controller Design

The Current controller ensures the operation of the above-described converter in a CC mode of operation. A PI controller is designed for current mode control. The design procedure is same as voltage controller which is explained earlier. While designing the controller the control-to-current transfer function is required which is derived in section 3.3.

3.5.2 V2G operation

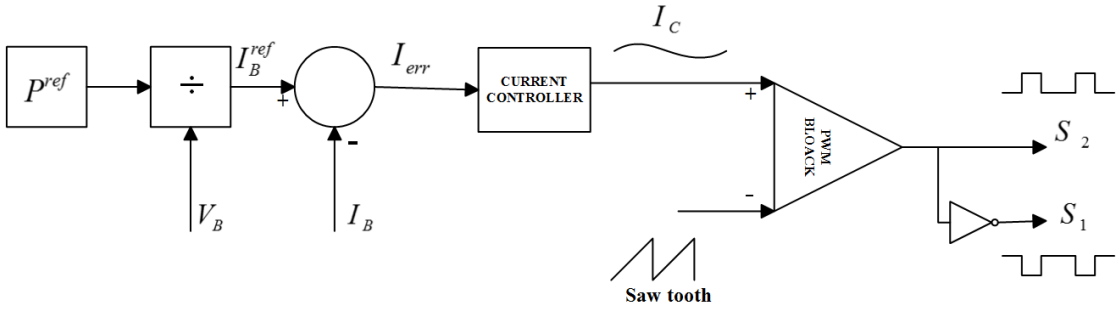

Fig 3.7 Controller for V2G mode

As described earlier in V2G mode the EV battery discharges to supply power in a reverse direction than can be fed back to the Grid or can be utilized for auxiliary battery charging purpose. Fig 3.7 shows a control structure for G2V operation. The objective of the controller is to deliver the desired amount of power from the traction battery to the Grid and Auxiliary battery. The amount of power that can be extracted from the battery is the reference power of the controller. The reference battery current is generated by dividing the reference power with the instantaneous battery voltage. The instantaneous battery current is compared with the reference battery current and the error acts as the input of the PI controller. Depending on the error the controller generates a gate driving pulses for both switches S_1 and S_2.As in the case of V2G mode, the DC-DC converter acts as a synchronous Boost converter the gate pulse is given to S_2 first whereas the complementary pulse is given to S_1.

3.6 Low-Voltage DC-DC Converter

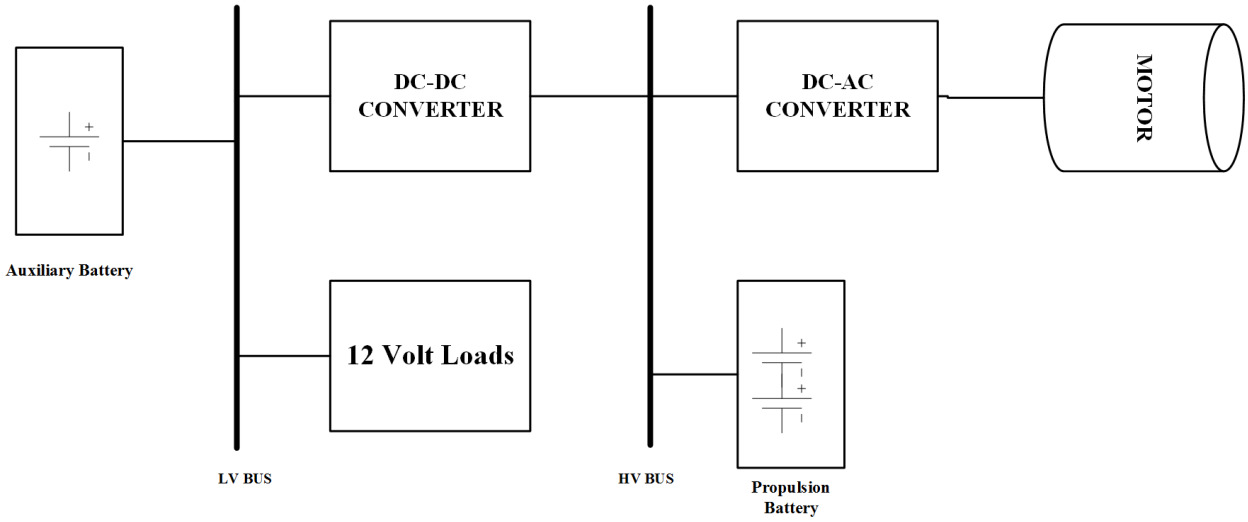

Fig 3.8 Block Diagram of Power distribution in EV

Every vehicle comprised of a low voltage battery (12 V) to supply low voltage loads i.e. lights, fan, music system etc. Conventionally an alternator is used to charge the low voltage battery in driving condition. The energy loss is more with the charging process because of energy conversion. As IC engine vehicles do not have any alternative to charging the low voltage battery hence the alternator cannot be omitted. EVs have the advantage that one High voltage battery pack is placed inside the vehicle for driving the vehicle i.e. propulsion battery. The low voltage battery i.e. Auxiliary battery can be charged from the propulsion battery directly and the alternator can be omitted by increasing the efficiency. A complete block diagram of different voltage levels is shown in Fig.3.8. The propulsion battery voltage varies usually in-between 150 to 600 V depending on the number of cells connected[22] .For driving purpose the battery voltage is converted into AC through a DC-AC converter. An LDC is required to charge the Auxiliary battery from the propulsion battery. A separate DC-DC converter can be employed to charge the low voltage battery or the same OBC can be employed to charge while in driving condition.AS the propulsion battery voltage is very high a forward converter with suitable transformer is a satisfactory option for LDC. The Auxiliary battery can supply energy to the HV Bus at starting. An isolated bidirectional converter can be employed for charging the low-voltage battery while driving and providing energy from the low voltage battery at starting operation. Additional converter leads to increase in cost and complexity of the vehicle. For level 1 charging the

charger is mounted on the vehicle itself .The OBC can serve the purpose of charging the auxiliary battery in a V2G or V2A (Vehicle to Auxiliary) manner [23]. The detailed operation of the proposed LDC is described below.

3.6.1 Power Stage Design and Operation of LDC

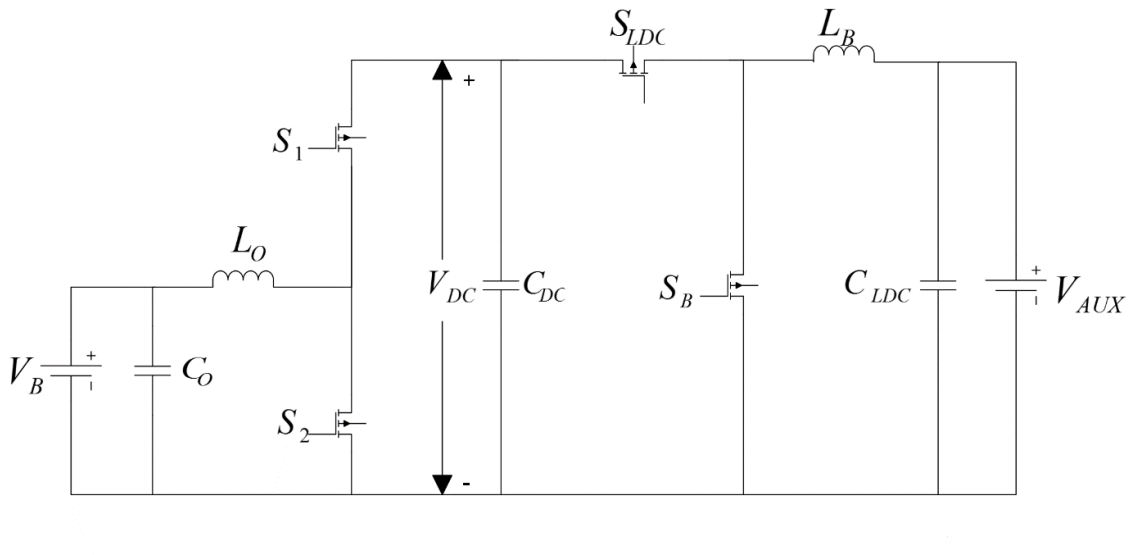

Fig 3.9 Low-Voltage DC-DC converter

An LDC is designed from the OBC and shown in Fig 3.9 and the diode bridge rectifier is omitted from the OBC as in Fig 1.2. The complete LDC can be divided into two parts. First, one is the synchronous DC-DC converter which is same as the converter explained in section 3.2 for V2G operation. The converter is operating as Boost converter to maintain 450 V across the DC link capacitor. The second stage is a synchronous Buck converter to step down the voltage level to 12 V for Auxiliary battery charging purpose. The second stage synchronous Buck converter is derived from the Boost PFC converter described in chapter 1 by allowing the power flow in reverse direction.

The operation of the converter is similar to cascades Buck-Boost converter. When S_2 and S_{LDC} is turned ON, S_1 and S_B are turned OFF as switches are synchronised with complementary gate pulse. Inductor L_O stores energy while DC link capacitor C_{DC} supplies power to the auxiliary battery via Boost inductorL_B.After first mode switches S_1 and S_B are turned ON and S_2 and S_{LDC} are turned OFF. The stored energy in the inductor and propulsion battery V_B both supply power to DC link and The Boost inductor energy freewheels via auxiliary battery and switchS_B [24][25].The inductor and capacitor values are same as designed before for each converter.

3.6.2 Controller Design of LDC

During driving condition the EV utilizes the energy of the propulsion battery and the voltage varies. As the Auxiliary battery is supplied from the propulsion battery the voltage of the auxiliary battery varies without a close loop controller. The purpose of the LDC controller to maintain 12 V across the auxiliary battery irrespective of the propulsion battery voltage.

The controller could be two stage controller by considering each converter individually. The first one to control the power from the propulsion battery as explained in section 3.5.2 in a G2V mode and the second one is a voltage control loop to maintain a constant voltage across the auxiliary battery. However, the control strategy is more complicated because of involvement of two controllers. A simple single stage control structure can be adopted to control both converters simultaneously. A voltage controller design the controls the two cascaded converters as one Buck converter. The controller can be designed as the procedure explained in section 3.5.1.1.

3.7 Simulation and Results

The described Non–Isolated Bi-directional DC-DC converter is simulated using MATLAB/Simulink for both G2V and V2G operation. Moreover, the Auxiliary Battery charging simulation is carried out using LDC. The detailed results are shown below.

3.7.1 G2V Mode

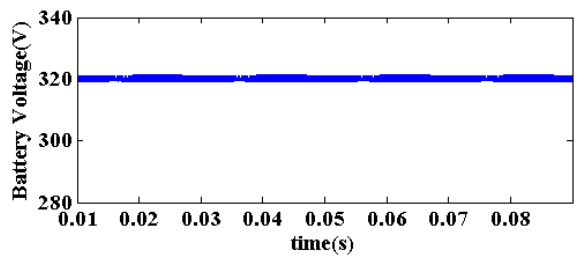

(a)

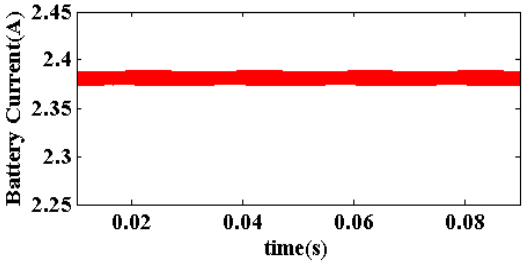

(b)

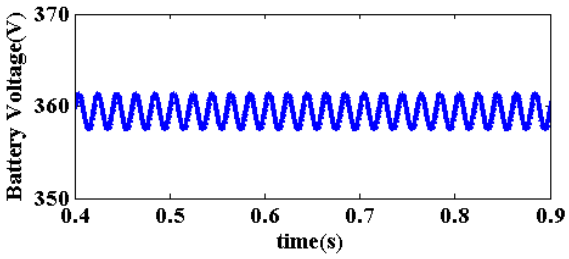

(c)

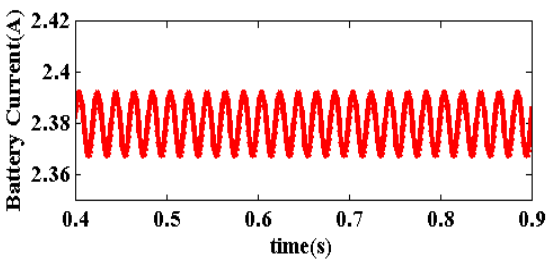

(d)

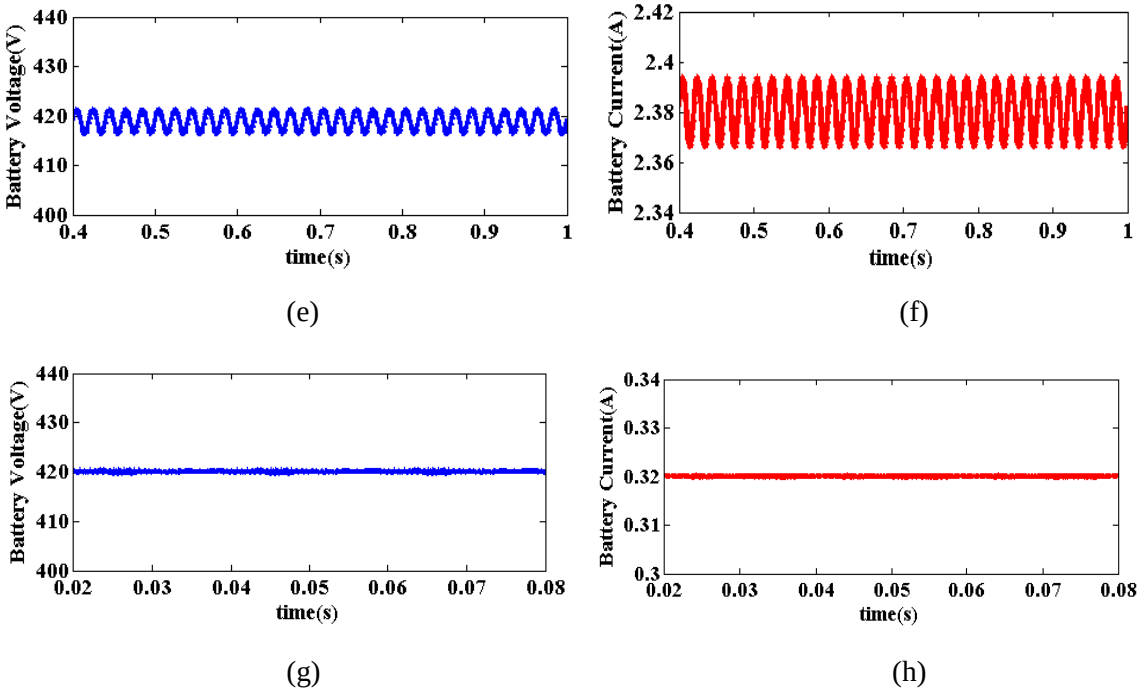

Fig 3.10 Simulated Results of Charging operation of the propulsion battery (a)Voltage and (b)Current in Beginning Point(c)voltage and (d)current in Nominal Point (e)voltage and (f)current in Turning Point(g)voltage and (h)current in End Point

Fig 3.10 shows the simulation results of G2V mode of operation. The results are emphasized on the four key points as described before. Simulation is performed by replacing the battery by its equivalent resistance which is the ratio of battery voltage to current. The depleted battery is charged from 320 V to maximum of 420 V via CC mode and then in CV mode till the battery current falls to 0.32 A. At the turning point the battery voltage reached to 420 V and the CC mode charging changes to CV mode. It can be verified from the simulation waveforms the battery current ripple is limited to 0.02 A peak-to-peak whereas the voltage ripple is limited to 3 V peak-to-peak.

3.7.2 V2G Mode

The V2G mode is simulated where the DC-DC converter acts as a Boost converter and supplies a desired amount of power to the DC link for further applications. The simulation is performed with a nominal battery voltage of 360 V and reference power of 800 Depending on the instantaneous battery voltage and reference power the controller generates a current reference and the switching of the two switches controlled in order to maintain the desired power flow.

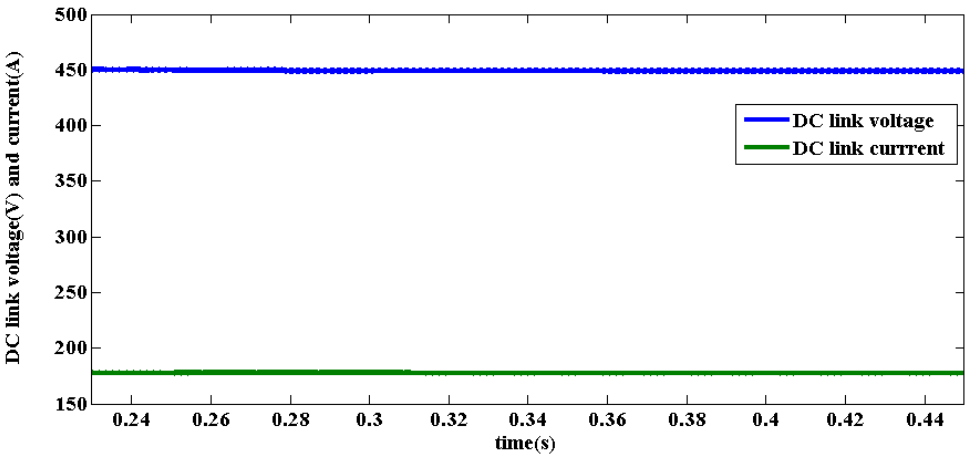

Fig 3.11 DC link voltage and current during G2V operation (The current is multiplied by 100 for batter visibility)

Fig 3.11 shows the simulated voltage and current waveform of the DC link when the power reference is 800 W. The DC link voltage is found to be 450 V as desired and the current is 1.78 A.

3.7.3 LDC

The simulation result in Fig 3.12 shows the Auxiliary battery voltage and current when the Auxiliary battery is charged from the propulsion battery via. LDC. The control strategy employed here is one stage controller as described in 3.6.2.The voltage of the battery is around 12 V with a small ripple of 0.1 V whereas the current is 1 A with negligible ripple. The propulsion battery is considered as in fully charged condition i.e. 420 V and all the power stage parameters are same as derived earlier.

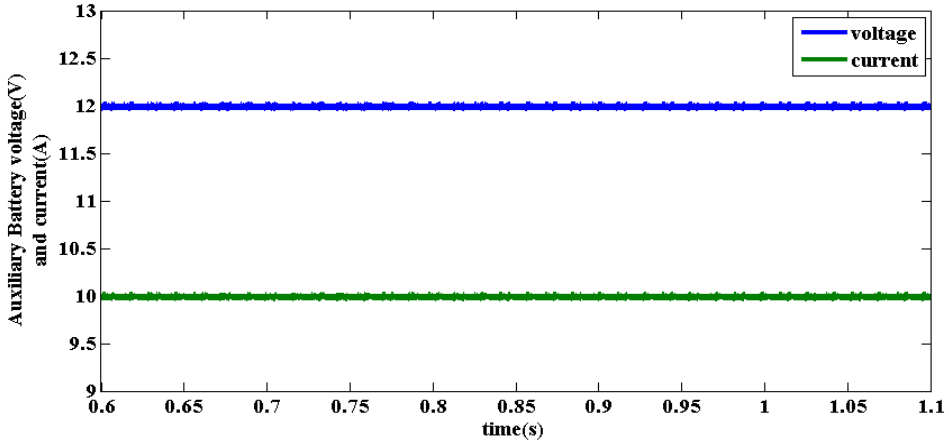

Fig 3.12 Voltage and Current of Auxiliary battery during charging

(Current is multiplied by 10 for better visibility)

3.8 Conclusion

The second stage of OBC i.e. DC-DC converter is essential as it regulates the battery voltage and current. The most common method of charging Li-Ion batteries i.e. CC/CV mode charging is obtained by using a DC-DC converter in this chapter. The Battery is charged from 320 V to 420 V in a CC manner with a constant current of 2.38 A and further in a CV manner by keeping the battery voltage fixed at 420 V. The designed DC-DC converter supports Bi-directional power flow and the V2G mode of operation is simulated with the V2G controller, a new concept of LDC is designed here by utilizing the OBC to charge in Auxiliary battery from the propulsion battery. A single stage controller is developed in order to maintain a desired voltage across the Auxiliary battery.

CHAPTER 4

CONCLUSION AND FUTURE SCOPE

4.1 Conclusion

An On-Board Electric Vehicle charger is designed for level 1 charging with a 230 V input supply. Different stages of an OBC is stated and the challenges are listed. The developments have been implemented to overcome key issues. A two stage charger topology with active PFC converter at the front end followed by a Bi-directional DC-DC converter is designed. The active PFC which is a Boost converter type produces less than 5 % THD at full load. Moreover, the PFC converter is applicable to wide variation in loads. The detailed design of the power stage, as well as the controller, is discussed with the simulated results.

A second stage DC-DC converter is designed and simulated for the charging current and voltage regulation. The converter performs very precisely by charging the propulsion battery in CC/CV mode over a wide range of voltage. A V2G controller has been developed for the DC-DC converter in order to supply power to the grid from the propulsion battery. A new Low-Voltage DC-DC converter is proposed to charge the Auxiliary battery via the propulsion battery utilizing the same OBC. The battery voltage and current waveforms are presented and the performance of the designed converter is verified.

4.2 Future Scope

The designed OBC is of two stage type whereas a single stage prototype can be designed which will reduce the losses associated with the components and maximize efficiency. Moreover, the Boost PFC converter is designed with an analogue controller the digital mode of the controller can be designed which can be implemented using microcontrollers.

A Bi-directional isolated DC-DC converter can be designed for both G2V and V2G modes and can operate as LDC. To reduce the switching losses a ZVS or ZCS topology of the designed DC-DC converter can be developed which will reduce the losses associated with the switches during turn ON or turn OFF.

REFERENCES

[1] "No Title," *https://en.wikipedia.org/wiki/Electric_vehicle*. .

[2] S. S. Williamson, *Energy management strategies for electric and plug-in hybrid electric vehicles*. Springer, 2013.

[3] a. Emadi and K. Rajashekara, "Power Electronics and Motor Drives in Electric, Hybrid Electric, and Plug-In Hybrid Electric Vehicles," *IEEE Trans. Ind. Electron.*, vol. 55, no. 6, pp. 2237–2245, 2008.

[4] M. Yilmaz and P. T. Krein, "Review of charging power levels and infrastructure for plug-in electric and hybrid vehicles," *2012 IEEE Int. Electr. Veh. Conf. IEVC 2012*, vol. 28, no. 5, pp. 2151–2169, 2012.

[5] H. Wang, S. Dusmez, and A. Khaligh, "Design and analysis of a full-bridge LLC-based PEV charger optimized for wide battery voltage range," *IEEE Trans. Veh. Technol.*, vol. 63, no. 4, pp. 1603–1613, 2014.

[6] P. Maheshwari, Y. Tambawala, H. S. V. S. K. Nunna, and S. Doolla, "A review of plug-in electric vehicles charging: Standards and impact on the distribution system," *Power Electronics, Drives and Energy Systems (PEDES), 2014 IEEE International Conference on*. pp. 1–6, 2014.

[7] S. K. Sul and S. J. Lee, "Integral battery charger for four-wheel drive electric vehicle," *IEEE Trans. Ind. Appl.*, vol. 31, no. 5, pp. 1096–1099, 1995.

[8] B. Whitaker, A. Barkley, Z. Cole, B. Passmore, D. Martin, T. R. McNutt, A. B. Lostetter, J. S. Lee, and K. Shiozaki, "A high-density, high efficiency, isolated on-board vehicle battery charger utilizing silicon carbide power devices," *IEEE Trans. Power Electron.*, vol. 29, no. 5, pp. 2606–2617, 2014.

[9] V. Monteiro, G. Pinto, and J. Afonso, "Operation Modes for the Electric Vehicle in Smart Grids and Smart Homes: Present and Proposed Modes," *IEEE Trans. Veh. Technol.*, vol. 9545, no. c, pp. 1–1, 2015.

[10] L. Solero, "Nonconventional on-board charger for electric vehicle propulsion batteries," *IEEE Trans. Veh. Technol.*, vol. 50, no. 1, pp. 144–149, 2001.

[11] T. Konjedic, L. Korosec, M. Truntic, C. Restrepo, M. Rodic, and M. Milanovic, "DCM-based Zero-Voltage Switching Control of a Bidirectional DC-DC Converter With Variable Switching Frequency," *IEEE Trans. Power Electron.*, vol. 31, no. 4, pp. 3273–3288, 2015.

[12] B. S. S. Singh, "Single-phase power factor controller topologies for permanent magnet brushless DC motor drives," no. October 2008, 2010.

[13] X. Wu, J. Yang, J. Zhang, and M. Xu, "Design considerations of soft-switched buck PFC converter with constant on-time (COT) control," *IEEE Trans. Power Electron.*, vol. 26, no. 11, pp. 3144–3152, 2011.

[14] J. Chen, D. Maksimović, and R. W. Erickson, "Analysis and design of a low-stress buck-boost converter in universal-input PFC applications," *IEEE Trans. Power Electron.*, vol. 21, no. 2, pp. 320–329, 2006.

[15] J. Arrillaga, B. C. Smith, N. R. Watson, and A. R. Wood, *Power system harmonic analysis*. 2013.

[16] D. Committee, I. Power, and E. Society, "IEEE Recommended Practice and Requirements for Harmonic Control in Electric Power Systems IEEE Power and Energy Society," vol. 2014, 2014.

[17] R. W. Erickson and D. Maksimovic, *Fundamentals of power electronics*. Springer Science & Business Media, 2007.

[18] S. Abdel-rahman, "PFC Boost Converter Design Guide," 2014.

[19] P. N. Ekemezie, "Design of a power factor correction ac-dc converter," in *AFRICON 2007*, 2007, pp. 1–8.

[20] W. Method, W. Ma, M. Wang, S. Liu, S. Li, and P. Yu, "Stabilizing the Average-Current-Mode-Controlled Boost PFC Converter via," vol. 58, no. 9, pp. 595–599, 2011.

[21] S. Choudhury, "Average current mode controlled power factor correction converter using TMS320LF2407A," *Appl. Note SPRA902A. Texas Instruments*, no. July, pp. 1–15, 2003.

[22] H. Plesko, J. Biela, J. Luomi, and J. W. Kolar, "Novel concepts for integrating the electric drive and auxiliary DC-DC converter for hybrid vehicles," *IEEE Trans. Power Electron.*, vol. 23, no. 6, pp. 3025–3034, 2008.

[23] S. Kim and F. S. Kang, "Multifunctional onboard battery charger for plug-in electric vehicles," *IEEE Trans. Ind. Electron.*, vol. 62, no. 6, pp. 3460–3472, 2015.

[24] M. A. Khan, I. Husain, and Y. Sozer, "A Bi - directional DC - DC Converter with Overlapping Input and Output Voltage Ranges and Vehicle to Grid Energy Transfer Capability," vol. 2, no. 3, pp. 507–516, 2014.

[25] M. A. Khan, I. Husain, and Y. Sozer, "A Bi - directional DC - DC Converter with Overlapping Input and Output Voltage Ranges and Vehicle to Grid Energy Transfer Capability."